Draft 11-17-2019 For BioRxiv

The a-isoform of $VEGFA_{165}$ is a Significantly Stronger Activator of Human Retinal Endothelial Cells compared to the b-isoform.

Wendelin Dailey[1], Roberto Shunemann[1,2], Fang Yang[1,3], Megan Moore[1], Austen Knapp[1], Peter Chen[1], Mrinalini Deshpande[1], Brandon Metcalf[1], Quentin Tompkins[1], Alvaro E. Guzman[1], Jennifer Felisky[1], Kenneth P. Mitton[1]*

1. Eye Research Institute, Oakland University, Rochester Michigan, USA
2. Currenty, Clinica Opthtalmus, Joinville – SC, Brazil
3. Currently Department of Ophthalmology, Renmin Hospital, Hubei University of Medicine, Shiyan, Hubei 442000,P.R. China.

Supported by National Eye Institute / National Institutes of Health (USA) grant NIH EY025089 (KPM).

*** Corresponding author.**
Kenneth P. Mitton, PhD FARVO
Associate Professor of Biomedical Sciences
Oakland University
mitton@oakland.edu
1-248-370-2079

Keywords: blood-retinal barrier, VEGFA165b, MAPK, AKT, Endothelial blood-retinal barrier, diabetic retinopathy, image analysis, optical coherence tomography, retinal cell culture, retinal vasculature

ABSTRACT

Studies show that the b-isoform of Vascular Endothelial Growth Factor-A-165 ($VEGFA_{165}b$) is predominant in normal human vitreous, switching to the a-isoform ($VEGFA_{165}a$) in the vitreous of eyes with active diabetic retinopathy or ROP. The potential of this isoform-switching to impact the retinal vasculature is not clear, particularly in endothelial cells which are important targets of VEGFA-mediated activation. We wished to determine if significant differences exist in the ability of these two isoforms to activate intracellular signalling and gene expression changes in retinal endothelial cells. Effects of $VEGFA_{165}$ isoforms (a/b) on the retinal vasculature were tested by intravitreal injection in rats using fluorescein-angiography and Optical Coherence Tomography to monitor primary vein dilation and retinal edema. Dose response curves for activation of MAPK (ERK1/2), AKT and VEGFR2 were determined using primary Human Retinal Microvascular Endothelial Cells (HRMECs). The ability of both isoforms to alter gene expression markers related to endothelial cell / leukocyte adhesion and tight-junctions was tested by quantitative-PCR. In rats, dilation of primary retinal veins and edema could be induced within 24 hours by intravitreal injection of sufficient amounts of either isoform. Both isoforms activated MAPK and AKT in primary HMRECs, however dose-response analysis revealed much stronger activation of MAPK, AKT and VEGFR2 by the a-isoform. The a-isoform was also more effective at increasing *ICAM1*, *VCAM1* and *SELE* gene expression and decreasing *CLDN5 and OCLN* gene expression in primary HRMECs. In conclusion, $VEGFA_{165}a$ could maximally activate the MAPK and AKT intracellular kinases in HRMECs at lower concentrations where $VEGFA_{165}b$ had little effect. Shifts of $VEGFA_{165}$ expression from mostly b-isoform to mostly a-isoform in some human retinal vascular diseases could potentially contribute to VEGFA-driven pathology through differential effects on the activation of retinal endothelial cells.

1. Introduction

Vascular Endothelial Growth Factor-A-165 ($VEGFA_{165}$) is the isoform of VEGF that is primarily responsible for driving retinal vascular pathology in diabetic retinopathy (DR), age-related macular degeneration (AMD) and retinopathy of prematurity (ROP), through activation of VEGF Receptor-2 (VEGFR2). A seminal analysis of the vitreous fluids of patients with diabetic retinopathy established the presence of elevated VEGF concentrations associated with this and other conditions (Aiello et al., 1994). That study contributed to the eventual development of intravitreal VEGF-blocking drugs to treat neovascularization and edema in AMD, DR, and the current exploration of their use for ROP (Amadio et al., 2016; Friedman, 2012; Miller et al., 1997; Robbins et al., 1997).

Blockade of VEGFA activity is provided by the use of intravitreal drugs including ranibizumab (Lucentis, Genentech), bevacizumab (Avastin, Genentech), pegaptanib (Macugen, Bausch & Lomb), and aflibercept (Eylea, Regeneron). Some VEGF-blocking drugs injected into the vitreous can enter the systemic circulation and, in the case of bevicizumab and aflibercept they can substantially decrease serum VEGF concentration for several days (Avery et al., 2014). Many non-endothelial cell types also express VEGF receptors such as neurons. VEGF receptors are also expressed by cells of the immune system, including early and late hematopoietic progenitor cells, dendritic cells, T-lymphocytes and macrophages (Li et al., 2016). Because VEGF is also essential for vascular health, there is interest to advance VEGF-regulating therapies by more precise titration of VEGF concentration or by modulating specific portions of VEGF-mediated signalling. Unfortunately, much published research does not differentiate between VEGFA's isoforms and in the case of retina there is less extensive investigation using primary

human retinal endothelial cells. This field of research would benefit from a more complete knowledge of VEGF's signaling mechanisms within endothelial cells.

Isoforms of the VEGFA protein result from transcriptional alternative-splicing of eight exons, which includes the alternative exons-8a and -8b (Bates et al., 2002; Ferrara, 2010; Park et al., 1993; Qiu et al., 2009). The most frequently detected isoforms are $VEGFA_{121}$, $VEGFA_{165}$ and $VEGFA_{189}$, with 121, 165 and 189 amino acids respectively. Other isoforms include 145, 162 and 183. One major functional impact of alternative splicing is to produce less diffusible isoforms like $VEGFA_{165}$, which includes a heparin-binding domain encoded by exon-7. $VEGFA_{189}$ and $VEGFA_{206}$ have even more affinity for heparin with an additional heparin-binding domain encoded by exon-6 (Ferrara, 2010; Park et al., 1993). $VEGFA_{121}$ is more diffusible, without any heparin-binding domains. All of these VEGFA isoforms bind as dimers to activate the receptor-tyrosine kinase, VEGFR2. $VEGFA_{165}$ also binds Neuropilin-1 as a co-receptor, while $VEGFA_{121}$ lacks the C-terminal regions required to bind Neuropilin-1. While $VEGFA_{165}$ and $VEGFA_{121}$ have similar binding affinities for VEGFR2, $VEGFA_{121}$ activates VEGFR2 less strongly than $VEGFA_{165}$. This was attributed to $VEGFA_{165}$'s ability to form a larger complex of multiple VEGFR2 dimers with additional involvement of Neuropilin-1 as a co-receptor (Whitaker et al., 2001).

The a- and b-isoforms differ in the sequence of their C-terminal six amino acids (Bates et al., 2002). This difference renders the b-isoform incapable of bringing the co-receptor Neuropilin-1 into a receptor/ligand complex with VEGFR2 (Prahst et al., 2008; Soker et al., 1998; Woolard et al., 2004). Similar to $VEGFA_{121}$, which only binds to VEGFR2, $VEGFA_{165}$b is

less angiogenic than the a-isoform (Bates et al., 2002; Konopatskaya et al., 2006; Magnussen et al., 2010). VEGFA$_{165}$b has similar VEGFR2-binding affinity as VEGFA$_{165}$a in Human Umbilical Vein Endothelial Cells (HUVECs). The b-isoform also displays weaker activation of VEGFR2 and ERK1/2 than the a-isoform in transfected porcine aortic endothelial (PAE) cells (Cébe Suarez et al., 2006). Perrin et al. (2005), detected a switch from mostly b-isoform to mostly a-isoform in the vitreous of patients with active diabetic retinopathy (Perrin et al., 2005). A similar shift, from VEGFA$_{165}$b to VEGFA$_{165}$a, was reported from analysis of vitreous humor of young patients with ROP (Zhao et al., 2015). An equivalent isoform switching of murine VEGFA$_{164}$a to VEGFA$_{164}$b occurs in a mouse model of oxygen-induced retinopathy (Zhao et al., 2011).

Intravitreal injection of VEGFA$_{165}$b was reported to reduce the leakiness of the retinal vasculature in one-week diabetic rats which suggested that the b-isoform could be beneficial by sequestering VEGFR2 signalling in a lower activated state (Ved et al., 2017). Here, we report that a relatively higher dose of VEGFA$_{165}$b was capable of dilating primary retinal veins to the same extent as VEGFA$_{165}$a in the normal rat eye. Both of these observations are compatible if there is a significant difference in the dose response effects of the two isoforms on retinal endothelial cells. We hypothesized that there is a significant difference in the dose-reponse for activation of retinal endothelial cells between the a- and b-isoforms of VEGFA$_{165}$. Furthermore we hypothesized that the a-isoform is a significantly stronger activator of VEGFA signalling pathways within this cell type. To address these hypotheses, we determined the dose-reponse for activation of MAPK (ERK1/2), AKT and VEGFR2 in primary HRMECs for both isoforms of VEGFA$_{165}$. Our results demonstrate that there is a significant difference in the ability of these two isoforms to activate intracellular signalling and change gene expression in primary human retinal endothelial cells.

2. Materials and methods

2.1. Cell Culture and Antibodies

Human Retinal Microvascular Endothelial Cells (HRMEC) and Attachment Factor were purchased from Cell Systems (Kirkland, WA). EndoGRO-MV Complete media kit was obtained from Millipore (Burlington, MA). EndoGro basal medium was supplemented with rhEGF, L-Glutamine, Heparin Sulfate and Ascorbic Acid according to the kit instructions. Additionally, supplementation with FBS and Hydrocortisone Hemisuccinate (1µg/ml) was dependent upon the assay requirements. Recombinant human $VEGFA_{165}a$ and $VEGFA_{165}b$ were obtained from R&D Systems (Minneapolis, MN). Odyssey Blocking Buffer and an Odyssey Infrared Imager were purchased from LI-COR Biosciences (Lincoln, NE). The antibodies used for in situ labeling of HMRECs (In Cell Westerns, ICW) and Western blotting are summarized in Table 1. Mini Protean TGX gels were purchased from Bio-Rad (Hercules, CA).

Table -1. Specific Antibodies used and Sources

Antibody	IgG Species	Company	Cat. No.
Phospho-AKT (P-Ser473)	Rabbit	Cell Signaling Technologies	4058
AKT(pan)	Rabbit	Cell Signaling Technologies	4691
Phospho-p44/42 MAPK (Thr202/204)	Rabbit	Cell Signaling Technologies	4370
p44/42 MAPK (pan)	Rabbit	Cell Signaling Technologies	4695
Phospho-VEGFR2 (Tyr1175)	Rabbit	Cell Signaling Technologies	2478
Beta-Actin	Mouse	Millipore	MAB1501
Anti-mouse IgG IRDye 800CW	Goat	LI-COR	32210
Anti-rabbit IgG IRDye 680RD	Goat	LI-COR	68071
Anti-rabbit IgG IRDye 800CW	Goat	LI-COR	32211
Anti-mouse IgG IRDye 680RD	Goat	LI-COR	68070

2.2. Animals

All experiments performed in this study were carried out with the approval of Oakland University's Animal Care and Use Committee and conformed to the ARVO Statement for the Use of Animals in Ophthalmic and Vision Research. Rats were housed at Oakland University in a facility approved by the Association for Assessment and Accreditation of Laboratory Animal Care International. Adult Long Evans rats (155-190 grams body weight, female) were obtained from Charles River Laboratories (Wilmington, MA).

2.3. Anesthesia for injections or retinal imaging

Pupils were dilated with tropicamide and phenylephrine drops prior to anesthesia. Rats were anesthetized with an intra-peritoneal injection of a Ketamine HCL (50 mg/kg) and Xylazine (7 mg/kg).

2.4. Evans Blue Angiography

Evans blue solution (30mg/ml) at a dose of 30 mg/kg was injected intravenously (tail vein) two hours prior to imaging for Evans Blue Angiography. After sedation and pupil dilation, retinas were imaged using a MICRON 3 camera system (Phoenix technology group, Pleasanton, CA) using the Evans Blue filter set (green illumination, red emission). Corneal surfaces were covered using GenTeal lubricant eye gel (Novartis, CVS Pharmacy) to prevent corneal dehydration and to provide optical transmission with the camera lens (rat).

2.5. Fluorescein Angiography

After sedation and pupil dilation, rats were injected (intra peritoneal) with 50 microliters of 10% sodium fluorescein in PBS. Retinas were imaged using a MICRON 3 camera system using the fluorescein filter set (blue illumination, green emission). Corneal surfaces were covered using GenTeal lubricant eye gel (Novartis, CVS Pharmacy) to prevent corneal dehydration and to provide optical transmission with the camera lens (rat).

2.6. $VEGFA_{165}a$ and $VEGFA_{165}b$ intravitreal injection (rat)

All animals were pre-imaged, prior to injections of VEGFA, using fluorescein angiography and SD-OCT imaging to record the status of their normal retinal vasculature. Both imaging modes were completed in a single session of anesthesia. This was typically performed about one week before intraocular injections with VEGFA isoforms. Rats were anesthetized and their pupils dilated prior to intraocular injections. Recombinant carrier-free human $VEGFA_{165}a$, or $VEGFA_{165}b$, was reconstituted with phosphate buffered saline solution (PBS, no calcium, no magnesium) to the appropriate concentration for intravitreal injections of a 5µl volume (dose 300 ng/eye). Injections were done with a NanoFil syringe fitted with 35 gage and beveled NanoFil needles (WPI Inc., Sarasota, Florida). The contralateral eye served as a control and received the same injection procedure-using vehicle alone (PBS). Depending on the experimental goal, imaging of the retinal vasculature was generally repeated at 24, 48, or 72 hours post injection and retinas collected for biochemical analysis.

2.7. Analysis of rat retinal edema and primary retinal vein diameter in vivo

Spectral Domain Optical Coherence Tomography (SD-OCT) was utilized to measure changes in retina thickness in vivo, induced by intravitreal injection of VEGFA isoforms. Retinal thickness was measured between the Inner Limiting Membrane (ILM) and the Outer Limiting Membrane (OLM) to detect potential retinal edema involving the neural retinal vasculature. To maintain corneal transparency, Artificial Tears lubricant eye drops (CVS Pharmacy) solution were applied generously to the both corneal surfaces during imaging. Anesthetized rats were secured in a three-axis positioning support cradle (Bioptigen, Durham NC). SD-OCT scans were taken using an Envisu R2200 model SD-OCT system (Bioptigen) equipped with a lens for the rat eye axial length. A rectangular scan pattern of rat sizes 2.6 mm x 2.6 mm was used (1000 A-scans by 100 B-scans). For measuring retinal vein thickness, calipers were positioned and locations recorded for subsequent re-measurements of the same primary veins locations after injection of VEGFA isoforms. For measurement of retinal edema, retinal layers were marked and measured using processed OCT images with *InVivoVue Diver* 2.0 software (Bioptigen) as previously described (Dailey et al, 2017). A fixed 5x5 grid was first centered on the optic disc. Boundaries of all retinal layers were marked at measurement grid locations. The central grid position was not used as it marks the optic disc center. The remaining 24 grid positions were then used to generate an average thickness between the inner limiting membrane and the outer limiting membrane for each eye, both pre- and post-injection.

2.8. Immunoblotting of activated MAPK and AKT in HRMECs

Primary Human Retinal Microvascular Endothelial Cells (HRMECs, genotype XY) were obtained from Cell Systems (Kirkland, WA, Catalog number: ACBRI-181). HRMECs were grown in 100mm dishes that had been pre-coated with Attachment Factor (Cell Systems, WA).

Media was EndoGRO (No VEGF, Millipore Sigma, Burlington, MA) with 5% FBS to establish confluency. When cells were confluent, the media was replaced with fresh media with or without $VEGFA_{165}$ isoforms. After incubation for 10 minutes, the cells were washed with ice cold PBS and the dishes were scraped to detach the cells. The cell suspension was then centrifuged at 1000 X g for 5 minutes and the cells were reconstituted in RIPA cell-lysis buffer (150 mM NaCl, 1% Triton-X-100, 0.1% SDS, 50 mM Tris, pH 8.0, 10 mM Sodium Fluoride, 1 mM Sodium Orthovanadate and complete Protease inhibitor cocktail (1 tablet/10 ml)). The cells were then sonicated or vortexed every 10 minutes while kept on ice for 30 minutes. The cell lysate was collected after centrifuging at 14,000 X g for 15 minutes at 4°C. The protein concentration was then measured using Pierce BCA Protein Assay (Thermo Scientific). The samples were then prepared with Laemmli sample buffer and loaded onto a (4-15%) gradient gels for SDS-PAGE electrophoresis. After electrophoresis the gels were equilibrated in cold transfer buffer and then transferred to PDVF membranes overnight. The membranes were then blocked with Odyssey blocking buffer and incubated with appropriates rabbit primary antibodies (Table-1) along with mouse monoclonal Actin antibody which was used for normalization. After washing with PBS, 0.1% tween-20 (4 X 5 min), the membranes were incubated with secondary antibodies (Goat Anti-rabbit IRDye680 and Goat Anti-mouse IRDye800CW) for 30-60 minutes. They were then washed and scanned on an Odyssey Infrared imager (Li-Cor, Lincoln, NE).

2.9. Dose-response analysis of intracellular signaling in primary HMRECs

HRMECs were seeded into black 96 well plates (5000/well) that had been coated with Attachment Factor. The cells were grown to confluence using fully supplemented EndoGRO-MV media for 4-5 days. The cells were then serum starved overnight using EndoGRO-MV

without Hydrocortisone. The cells were treated with $VEGFA_{165}a$ or $VEGFA_{165}b$ for varied lengths of time after which the treatments were immediately removed and replaced with of 4% Paraformaldehyde. The cells were fixed for 20 minutes at room temperature followed by permeabilization with PBS, 0.1% Triton X-100 (10 minutes). The cells were then blocked by incubation with Odyssey Blocking Buffer (Li-Cor) for 1.5 hours at room temperature and then incubated with primary antibodies (1:200) for either 2 hours at room temperature or over night at 4 °C. Rabbit antibodies were used against the proteins of interest and a mouse monoclonal anti-Beta-Actin antibody was used for normalization. The cells were then washed with PBS, 0.1% Tween 20 (5x5 minutes) and incubated with secondary antibodies, Goat anti-Rabbit IRDye 800CW & Goat anti-Mouse IRDye 680RD (1:750) for 45 minutes at room temperature. After washing with PBS 0.1% Tween 20 (5x5 minutes) the plates were scanned on an Odyssey Imager (Li-Cor). For time response and dose response experiments, the doses of $VEGFA_{165}a$ and $VEGFA_{165}b$ were assayed in quadruplicate wells and dose response experiments were repeated three times to confirm reproducibility of relative dose reponse differences for activation of MAPK (phospho-Thr202/Tyr204), AKT (phospho-Ser473) and VEGFR2 (phospho-Tyr1175).

2.10. Quantitative PCR analysis of HMREC Gene Expression

Primary HMRECs were grown to confluence in six well plates. After the desired treatment, cells were trypsinized. Total RNA was isolated using the Absolutely RNA miniprep kit (Agilent, Santa Clara, CA). Cells were homogenized in 200µL of lysis buffer. Homogenization was accomplished using conical pellet-pestles in 1.5 mL microfuge tubes, with a hand-held rotary tool (Bel-Art,Wayne, NJ). First-strand cDNA was synthesized by reverse transcribing 500 ng of total RNA per sample using either the AffinityScript qPCR DNA Synthesis kit (Agilent), or the

LunaScript RT Super Mix Kit (NEB # E3010(S/L), Ipswich, MA) with Oligo-dT priming. The reaction conditions were according to the manufacturer's instructions. For AffinityScript: 25ºC for 5 min, 42ºC for 20 min, 95ºC for 5 min, and 10ºC for 10 min. For LunaScript RT: 25ºC for 2 min, 55ºC for 10 min, and 95ºC for 1 min. All compared samples were processed using the same reagent set. Stock first strand cDNA preparations were stored at -70°C, and were not used for analysis after a maximum of three freeze-thaws. Duplex reaction format was utilized with FAM-labeled probe/primer pairs for the gene of interest and VIC-labeled probe/primer-limited pairs for TBP (Tata-Binding Protein) as the normalizer gene (ThermoFisher, Waltham, MA). For real-time PCR reactions, sample first-strand cDNA was diluted 5-fold with deionized water and 2µL added to 18µL of master mix for 20µL PCR reactions. Triplicate reactions were used for each sample. Master Mix chemistries were either 2x Gene Expression Master Mix (ThermoFisher, Applied Biosystems # 4369016, Waltham, MA), or the Luna Universal Probe qPCR Master Mix (2x) Gene Expression (New England BioLabs # M3004L, Ipswich, MA), both mixes with the Rox reference dye option. Reactions were run on either an Mx3000P real-time PCR system using the MxPro software, or an AriaMx Real-time PCR System using the AriaMx HRM QPCR Software (Agilent, *Santa Clara, CA)*. Gene expression assays were evaluated for high PCR efficiency using a dilution series of HMREC cDNA to ensure validity of using the delta-delta Ct method for comparing relative gene expression. Each replicate reaction was internally normalized relative to endogenous TBP gene expression. The specific assay probe sets used for gene expression analysis are listed in Table 2.

Table 2. Taqman gene expression probes for HRMEC gene expression.

Gene	Probe Set #	Spans Exons
CLDN5	Hs01561351_m1	1-2
ICAM1	Hs00164932_m1	2-3
OCLN	Hs00170162_m1	5-6
SELE	Hs00174057_m1	4-5
TBP	Hs00427620_m1	3-4
VCAM1	Hs01003372_m1	6-7

3. RESULTS

3.1. Effects of $VEGFA_{165}a$ and $VEGFA_{165}b$ on the Retinal Vasculature In Vivo.

The Long Evans's rat strain was used for two reasons. First, to avoid the use of non-pigmented eyes, which may experience additional contributions from oxidation damage. Second, to allow the use of angiography for imaging the retinal vasculature, because this imaging mode is not possible with non-pigmented eyes. Intra-vitreal injection of $VEGFA_{165}$ isoforms were employed, as this method was used previously to demonstrate that VEGFA disrupts the blood retinal barrier and that VEGFA-blockade could be employed as a therapeutic strategy (Adamis et al., 1996; Aiello et al., 1995; Ozaki et al., 2000; Robinson et al., 1996; Xu et al., 2001).

Using fluorescein angiography and SD-OCT, the retinal vasculature was imaged prior to injections to allow comparison of the same retina after injections. This was the best way to account for the individual variation between rats for primary vein diameters as well as the individual pattern of each eye's vascular network. The contralateral eye served as an injected control, receiving the same injected volume of vehicle. Both isoforms of $VEGFA_{165}$ caused

visible dilation of the primary veins, which was not seen with the contralateral vehicle-injected eye. (**Figure-1**) Dilation of the primary retinal veins was maximum about 24 hours post-injection, followed by gradual recovery. Intraocular pressure was not elevated nor decreased, checked as early as 10 minutes after injections, and remained normal on subsequent days (data not shown). **Figure-2** shows another example of the dilation effect using the $VEGFA_{165}b$ isoform, as visualized using fluorescein angiography and SD-OCT imaging. Dilation of the primary veins was apparent at 24 hours post-injection and reverted almost to normal by 72 hours.

While injections with vehicle did not cause dilation of the primary veins, another control was demonstrated using Aflibercept to block the effect of $VEGFA_{165}b$ *in vivo* (**Figure-3**). Aflibercept is a recombinant VEGF-trap that contains the VEGF-binding sites of VEGFR2 and VEGFR1 and should be capable of blocking both $VEGFA_{165}a$ and $VEGFA_{165}b$ because they have the same binding affinity for VEGFR2. Fluorescein angiography of the $VEGFA_{165}b$ injected eye showed dilation of the primary retinal veins at 24 hours post injection, which was then decreasing by 48 hours. Aflibercept co-injection of the contralateral eye completely prevented dilation of primary retinal veins by $VEGFA_{165}b$ injection.

In another different experiment, Long Evans rats were also injected with $VEGFA_{165}a$ or $VEGFA_{165}b$ (300 ng) in one eye (OD) and the contralateral eye (OS) received an injection of the vehicle alone (PBS). SD-OCT imaging and Evans Blue angiography were employed to monitor for evidence of retinal edema. Fluorescein angiography images and 3D SD-OCT image data were obtained several days prior to intravitreal injections to provide individual starting baseline data

for all eyes. 24-hours after injections, all eyes were imaged again using Evans Blue angiography and 3D SD-OCT imaging.

Using 3D SD-OCT data sets, we measured changes in the diameter of primary retinal veins and changes in retinal thickness. Several primary veins were measured at the same location in retinas before injection and 24 hours post-injection. The average percent changes in vein diameter from before to after injection were compared for the VEGFA-injected eyes (OD) and also for the contralateral PBS-injected eyes. (**Figure-4**) $VEGFA_{165}a$ caused a 72% increase in average primary vein diameter, 24 hours post-injection. This was substantially larger than the average percentage change in diameters measured for the contralateral vehicle-injected control eyes ($P<0.005$, t-test). Similarly, a substantial increase in primary vein diameter of 54% was elicited by treatment with $VEGFA_{165}b$. This was significantly larger than primary vein diameter changes in the contralateral control eyes ($P<0.03$, t-test).

SD-OCT data was also processed using DIVER software to orient a 5x5 reference grid, centered on the optic disc, and the depth of all retinal layers were measured at 24 locations per retina. (The center position of the grid, on the optic disc, was not used for measurement.) For purposes of comparing changes that result from retina edema, the average thickness between the Inner-Limiting-Membrane (ILM) and the Outer-Limiting-Membrane (OLM) were calculated (**Figure-5**). First, the total average ILM-OLM thickness was calculated using all 24 grid locations. Additionally, central averages were calculated using only the 8 grid locations nearest the disc, and mid-peripheral averages were calculated using the outer 16 grid locations farther from the center. Both $VEGFA_{165}a$ and $VEGFA_{165}b$ caused a significant increase in ILM-OLM

thickness by 24 hours post-injection. Vehicle-injected contralateral eyes did not display significant changes in average ILM-OLM thickness. Significant increases in thickness were found in both the more central and more mid-peripheral zones.

Evans Blue angiography images were also captured for these same eyes that were measured by OCT for changes in retinal vein diameter and retinal thickness above. Evans Blue dye was delivered intravenous and permitted to circulate for 2 hours prior to imaging. At 24 hours post-injection, the $VEGFA_{165}$-injected eyes (OD) of all rats displayed the presence of intense vitreal Evans Blue fluorescence (red) using either isoform, which obscured the ability to visualize even the primary retinal vessels. An example is shown for both $VEGFA_{165}$a and $VEGFA_{165}$b injected eyes. (**Figure-6**) The contralateral PBS-injected eyes had far less vitreal-fluorescence and the primary and secondary retinal vessels could be imaged.

3.2. Activation of MAPK and AKT in primary HRMECs by $VEGFA_{165}$a and $VEGFA_{165}$b

To examine the effect of $VEGF_{165}$ isoforms on intracellular signaling pathways we chose primary human retinal microvascular endothelial cells (HRMECs) and tested for activation of the MAPK and AKT pathways. These pathways were examined as two of the intracellular signaling kinases implicated in mediating the effects of VEGFA on endothelial proliferation and blood-retinal barrier. We initially compared the ability of the a-isoform and the b-isoform to activate MAPK (ERK1/2) and AKT by immunoblotting. Using a relatively high dose (100 ng/mL, 5300 pM), both isoforms of $VEGFA_{165}$ increased the amounts of the active form of MAPK (**Figure-7a**) and the active form of AKT (**Figure-7b**), by about 2.7-fold and 1.6-fold (**Figure-7c**) respectively.

3.3 MAPK Activation by VEGFA$_{165}$a and VEGFA$_{165}$b: Timing and Dose-Response

Activation of the MAPK pathway in HRMECs occurred maximally at 10 minutes for both VEGFA$_{165}$a and VEGFA$_{165}$b treatment, and returned to control levels by 90 minutes, using a dose of 100 pM (**Figure-8a**). For the timed experiment, cells had 5% serum in basal medium. The activation by VEGFA165a was significantly stronger than that of VEGFA$_{165}$b ($P<0.01$).

We next carried out dose-response analysis for the activation of the MAPK (ERK1/2) using the 10 minutes time point and cells pre-adapated to lower serum. Eleven doses of each isoform were evaluated and dose-response data for MAPK activation were fit to the Log-Logistic 4-parameter dose-response function (Ritz et al., 2015). (**Figure-8b**) Activation of MAPK by VEGFA$_{165}$b showed a typical sigmoidal dose-response. Compared to VEGFA$_{165}$b, the dose-response curve for VEGFA$_{165}$a displayed a strong allosteric shift to a more binary-like activation response. The a-isoform was more potent for activation of MAPK at lower doses. A similar maximum level of MAPK activation could be achieved with the highest dose tested (10,000 pM) using either isoform. Activation of MAPK by 250 pM VEGFA$_{165}$b was only 10% of the maximum activation, which was generated by VEGFA$_{165}$a treatment at this dose. The ED_{50} dose was 73 pM for VEGFA$_{165}$a and 1015 pM for VEGFA$_{165}$b for the experiment shown. The experiment was repeated three times confirm the reproducibility of this large difference in dose-response between the two isoforms. Differences between the ED_{50} values were typically in the 800 to 1000 pM range.

3.4. AKT Activation by VEGFA$_{165}$a and VEGFA$_{165}$b: Timing and Dose-Response.

Maximum activation of the pAKT pathway in HRMECs occurred between 15 and 30 minutes for VEGFA$_{165}$a treatment and VEGFA$_{165}$b treatment (**Figure-9a**). Dose response analysis was then carried out for AKT activation using these maximum time points of response (**Figure-9b**). With VEGFA$_{165}$a, AKT activation in HRECs displayed a much steeper dose-response curve than for VEGFA$_{165}$b. The ED$_{50}$ doses were 53 pM for VEGFA$_{165}$a compared to 126 pM for VEGFA$_{165}$b. In addition, the maximum activation of AKT generated by the b-isoform was less than half that obtained from treatment with the a-isoform. Repetition of the experiment confirmed similar relative responses.

3.5. VEGFR2 Activation by VEGFA$_{165}$a and VEGFA$_{165}$b: Dose-Response

Hypothetically, the differences in activation of the MAPK and AKT kinases can begin upstream at the activation of the VEGFR2 receptor. To determine if the relative difference in dose-response kinetics might begin at the level of the receptor itself we examined the dose-response for activation of VEGFR2. Maximum activation of the receptor was very fast and likely within less than a few minutes (as quickly as cells could be processed for treatment and fixation). Five and ten minute experiments were similar in relative response, so ten minutes were used for the dose-response experiment shown. (**Figure-10a**). VEGFA$_{165}$a treatment achieved maximum activation by about 500 pM whereas the b-isoform caused little if any activation at that dose. The ED$_{50}$ for activation by the a-isoform was 254 pM compared to 1192 pM for the b-isoform. Furthermore, the maximum activation by the b-isoform was 73% of that obtained by the a-isoform. Again, this relative pattern was confirmed by a repeated experiment (data not shown).

3.6. Isoform Effects on Gene Expression: Leukocyte Docking and Tight-Junction Proteins

After establishing that the b-isoform was also capable of activating both MAPK and AKT, we examined several gene expression markers from 1 to 24 hours after $VEGFA_{165}$ treatment using a dose that provided for maximal activation of singalling by either isoform (5,300 pM). We examined three genes important for the activation of leukocyte-endothelial cell adhesion: *ICAM1*, *Selectin-E*, and *VCAM1* (**Figure-11a, c, e**). All three of these genes displayed increased expression after treatment with either isoforms of $VEGFA_{165}$ with maximum changes at the 6 hour point. These trends were confirmed by repeated experiments. *ICAM1*'s increasing expression trend was the same but not always maximum at 6 hours, sometimes later by 24 hours (data not shown).

Guided by our kinase activation dose-response data, we selected a low (100 pM), intermediate (1000 pM) and high (5,000 pM) dose to test for dose-response differences in the relative activation of VEGFR2, MAPK and AKT. (**Figure-11b, d, f**). We used the 6 hour time point as most of the genes examined had shown substantial expression changes by that time. For all three leukocyte docking protein genes (*ICAM1*, *SELE*, *VCAM1*), $VEGFA_{165}$a increased their expression at the intermediate dose of 1000 pM where $VEGFA_{165}$b still had very little effect. Furthermore the b-isoform could not increase the expression of these three genes to the maxium level observed with the a-isoform.

We also compared the effects $VEGFA_{165}$ isoforms on the expression of genes encoding the tight-junction proteins Claudin-5 and Occludin (**Figure-12**). Both isoforms of $VEGFA_{165}$ reduced the expression of these genes with the stronger effect on *Claudin-5* gene expression.

Expression of both genes recovered by 24 hours (**Figure-12a, c**). Comparing the low, intermediate and high doses at 6 hours, $VEGFA_{165}b$ was also less effective at suppressing the expression of *Claudin-5* and *Occludin* compared to $VEGFA_{165}a$ (**Figure-12b, d**).

4. DISCUSSION

While the role of VEGFA in vascular development, tumorgenesis and hypoxia has been studied for over two decades, most studies have not differentiated the functional contributions of different VEGFA size-isoforms nor the a- and b-isoforms. More recently, isoform-specific analysis found that most $VEGFA_{165}$ in normal vitreous was the b-isoform, with the ratio changing to mostly a-isoform in eyes with active diabetic retinopathy and ROP (Perrin et al., 2005; Zhao et al., 2015). The a- and b-isoforms are both derived from the *VEGFA* gene through alternative splicing of the pre-mRNA. Phosphorylation of the ASF/SF2 splice-factor by the SR protein kinases (SRPK1/2) regulates alternate splicing of exon 8 to change from $VEGFA_{165}b$ mRNA to $VEGFA_{165}a$ mRNA (Nowak et al., 2010). An obvious question arises about whether this shift alters the functional effects of any concentration of $VEGFA_{165}$ on the retinal vasculature? That it could is a reasonable hypothesis because the change in isoform ratio is large.

We started our investigations by using intravitreal injections of what we estimated to be a substantial dose of either isoform in a pigmented rat model to determining if the b-isoform can affect the retinal vasculature similar to the a-isoform. While $VEGFA_{165}b$ does not bind the Neuropilin-1 co-receptor, it does bind to VEGFR2 with the same affinity as the a-isoform (Cébe Suarez et al., 2006). We found that both isoforms of $VEGFA_{165}$ could dilate primary retinal veins, an effect previously observed for $VEGFA_{165}a$ during studies that established it as a key disruptor

of the blood-retinal barrier (Aiello et al., 1997). This substantial dilation of primary veins (60%) recovered to normal over a few days. Both isoforms bind to the VEGFR2 receptor with similar affinity, and so the VEGF-trap Afliberept should block the dilation effect of the the b-isoform and that was the case.

Retinal edema was also observed using SD-OCT data. Again, both isoforms could increased ILM-OLM thickness. Consistent with the primary-vein dilation and edema, the a-isoform and the b-isoform also caused increased leakage of intravenous Evans Blue dye into the vitreous of VEGFA-injected eyes compared to contralateral vehicle–injected eyes. We concluded that the b-isoform of $VEGFA_{165}$ was capable of driving similar effects as reported for the a-isoform if injected in sufficient quantity. This result seemed like it might be contrary to the previous study where a lower dose of $VEGFA_{165}$b was reported to reduce the leakiness of the retinal vasculature in one-week diabetic rats, presumably by sequestering VEGFR2 signalling in a lower activated state (Ved et al., 2017). However, all of these observations would be compatable with the hypothesis that the b-isoform is a weaker activator of VEGF-mediated signaling in vascular endothelial cells compared to the a-isoform. Does-response curves would provide the answer. While it may be surprising in the age of anti-VEGF drug treatment, dose-response data comparing isoforms of VEGFA is sparse. We decided to examine isoform-specific activation using primary human retinal endothelial cells because results from non-retinal endothelia cells might not apply to the high-barrier endothelial cells of the CNS. Furthermore, we wanted to compare the effects of these two isoforms on the activation of intracellular signaling pathways, since binding assays would not inform us about the actual activation state of the endothelial cells.

Previous studies with procine aortic endothelial cells found that the a-isoform can activate the VEGFR2 receptor stronger than the b-isoform (Kawamura et al., 2008). Another study of human pulmonary microvascular endothelial cells (HPMECs) found that the a-isoform was a stronger activator of VEGFR2 and MAPK (ERK1/2) than the b-isoform at a dose of 20 ng/ml (1000 pM) (Ourradi et al., 2017). So we also began with immunoblotting to examine the activation of MAPK and AKT in primary HRMECs. We found that both MAPK and AKT were activated to a similar extent using a higher dose (100 ng/ml, 5,300 pM) in primary HRMECs. We found that both MAPK and AKT were activated less by the b-isoform at the lower dose (20 ng/ml, 1000 pM) (data not shown). With this preliminary guidance, we moved to use the in-cell-western (ICW) method to measure activation of these kinases *in situ*. This enabled us to explore activation in the form of complete dose response curves using many doses and replicate doses.

Our full dose-response curves confirmed that there are substantial differences in the activation of both MAPK and AKT by the two isoforms of $VEGFA_{165}$. In the case of MAPK, the ED_{50} dose (Effective Dose for 50% maximal activation) was over 800 pM lower for $VEGFA_{165}$a compared to the b-isoform. Higher doses of the b-isoform could activate MAPK to a similar maximum level, but it was apparent that $VEGFA_{165}$a caused maximum activation at far lower doses where $VEGFA_{165}$b had little effect. For AKT, the ED_{50} was two-fold greater for the b-isoform compared to the a-isoform. The activation of AKT by b-isoform remained subtanially less than that from the a-isoform over the entire dose-response range. In contrast to MAPK activtion, the maximum activation of AKT obtained with the b-isoform was half of the maximum using the a-isoform. This is at least one difference from human pulmonary endothelial cells where AKT activation was the same with both isoforms at a dose of 20 ng/ml (1000pM) (Ourradi et al.,

2017). This difference reveals that nuances of VEGF-mediated signaling should not be considered universal between different sub-types of vascular endothelial cells.

The necessity of studying primary HRMECs to properly understand the functional effects of VEGF isoforms in the neural retina is also supported by other studies. A recombinant protein (rVEGF$_{164}$b), modified from murine VEGF$_{164}$b, attenuated the VEGF$_{164}$a-induced proliferation of an *ImmortoMouse*-derived vascular endothelial cell line (MVEC), and reduced the VEGF$_{164}$**a**-induced disruption of an MVEC endothelia-cell barrier (Cromer et al., 2010). Similar to human VEGFA$_{165}$a and VEGFA$_{165}$b, murine VEGF$_{164}$a and the modified rVEGF$_{164}$b are different in their C-terminal amino acid sequence and this results in different functionality. Other studies with rVEGF$_{164}$b also indicate that the effects of the b-isoforms may be organ-specific, possibly dose-dependent, and require investigations for different organs and tissues. While viral delivery of rVEGF$_{164}$b attenuated inflammatory-response damage in a murine model of ulcerative colitis, it exacerbated blood-brain-barrier damage in a murine model of focal cerebral ischemia (Chaitanya et al., 2013; Cromer et al., 2013).

The hypothesis that the differences in the activation of MAPK and AKT begin with activation of the receptor was confirmed by our dose-response analysis for activation of VEGFR2. Again, the a-isoform was far more potent for activating VEGFR2 compared to the b-isoform. Altogether, our dose-response curves for the activation of VEGFR2, MAPK, and AKT are consistent with the model proposed by Whitaker et al., wherein the a-isoform activates VEGFR2 more intensely when it can bind the co-receptor Neuropilin-1 to form a larger activation complex comprised of more VEGFR2 and Neuropilin-1 subunits (Whitaker et al., 2001).

Consistent with our findings here that the b-isoform was also capable of activating both MAPK and AKT, we also found that $VEGFA_{165}b$ could affect the expression of genes regulated by $VEGFA_{165}a$. These included genes involved in leukocyte-endothelial cell adhesion and in tight-junction structure. VEGFA-mediated activation of the VEGFR2 receptor is known to disrupt adherin-junctions and causes ß-Catenin mediated repression of *Claudin-5* gene expression in endothelial cells (Taddei et al., 2008). We found that the *Claudin-5* gene was particulary succeptible to repression by both isoforms of $VEGFA_{165}$ compared to *Occludin* in this cell type. With guidance from our dose-response curves for kinase activation we were able to select several doses to ask: are differences in the relative activation of VEGFR2, MAPK and AKT translated into dose-response differences in gene expression? The answer to this question was yes. For all three leukocyte docking protein genes (*ICAM1, SELE, VCAM1*), $VEGFA_{165}a$ increased their expression at the intermediate dose of 1000 pM where $VEGFA_{165}b$ had very little effect. Furthermore the b-isoform could not increase the expression of these three genes to the level observed with the a-isoform. $VEGFA_{165}b$ was also less effective than the a-isoform at suppressing the expression of the tight-junction structural genes, *Claudin-5* and *Occludin*. We concluded that there were significant dose-response differences in the regulation of VEGFA-target genes, with the a-isoform proving to be the stronger affector of gene expression changes in primary HRMECs.

5. Summary

It is apparent that the b-isoform of $VEGFA_{165}$ was capable of affecting the rat retinal vasculature and activating primary HRMECs similar to the a-isoform. However, our dose-

response analysis found a substantial difference in the ability of these two isoforms to activate intracellular signaling in primary human retinal endothelial cells. This kinetic difference begins with the activation of VEGFR2 itself and propagates to differential activation of at least two important regulatory kinases in endothelial cells: MAPK (ERK1/2) and AKT. These dose-response effects are transmitted all the way to the expression of VEGFA-target genes involved in leukocyte endothelial cell adhesion and endothelial-cell tight junctions. Our results suggest that the expression switch from $VEGFA_{165}b$ to $VEGFA_{165}a$ reported in active DR and ROP vitreous could be a significant factor affecting retinal endothelial cells *in vivo*, and that this possibility warrants more investigation. If true, then inhibiting disease-related switching to expression of $VEGFA_{165}a$ would also be a potential target for therapeutic development.

Acknowledgements

The authors would like to thank Oakland University undergraduate students Regan Miller and Anju Thomas for assistance with some cell culture and some testing of gene expression probesets used for these studies. Research supported by National Eye Institute / National Institutes of Health (USA) grant NIH EY025089 (to KPM).

References

Adamis, A.P., Shima, D.T., Tolentino, M.J., Gragoudas, E.S., Ferrara, N., Folkman, J., D'Amore, P.A., Miller, J.W., 1996. Inhibition of vascular endothelial growth factor prevents retinal ischemia-associated iris neovascularization in a nonhuman primate. Arch. Ophthalmol. 114, 66–71. doi:10.1001/archopht.1996.01100130062010

Aiello, L.P., Avery, R.L., Arrigg, P.G., Keyt, B.A., Jampel, H.D., Shah, S.T., Pasquale, L.R., Thieme, H., Iwamoto, M.A., Park, J.E., 1994. Vascular endothelial growth factor in ocular fluid of patients with diabetic retinopathy and other retinal disorders. N. Engl. J. Med. 331, 1480–7. doi:10.1056/NEJM199412013312203

Aiello, L.P., Bursell, S.E., Clermont, A., Duh, E., Ishii, H., Takagi, C., Mori, F., Ciulla, T.A., Ways, K., Jirousek, M., Smith, L.E.H., King, G.L., 1997. Vascular endothelial growth factor-induced retinal permeability is mediated by protein kinase C in vivo and suppressed by an orally effective β-isoform-selective inhibitor. Diabetes 46, 1473–1480. doi:10.2337/diab.46.9.1473

Aiello, L.P., Pierce, E.A., Foley, E.D., Takagi, H., Chen, H., Riddle, L., Ferrara, N., King, G.L., Smith, L.E., 1995. Suppression of retinal neovascularization in vivo by inhibition of vascular endothelial growth factor (VEGF) using soluble VEGF-receptor chimeric proteins. Proc. Natl. Acad. Sci. U. S. A. 92, 10457–61. doi:10.1073/PNAS.92.23.10457

Amadio, M., Govoni, S., Pascale, A., 2016. Targeting VEGF in eye neovascularization: What's new?: A comprehensive review on current therapies and oligonucleotide-based interventions under development. Pharmacol. Res. doi:10.1016/j.phrs.2015.11.027

Avery, R.L., Castellarin, A.A., Steinle, N.C., Dhoot, D.S., Pieramici, D.J., See, R., Couvillion, S., Nasir, M.A., Rabena, M.D., Le, K., Maia, M., Visich, J.E., 2014. Systemic pharmacokinetics following intravitreal injections of ranibizumab, bevacizumab or aflibercept in patients with neovascular amd. Br. J. Ophthalmol. 98, 1636–1641. doi:10.1136/bjophthalmol-2014-305252

Bates, D.O., Cui, T.G., Doughty, J.M., Winkler, M., Sugiono, M., Shields, J.D., Peat, D., Gillatt, D., Harper, S.J., 2002. VEGF165b, an inhibitory splice variant of vascular endothelial growth factor, is down-regulated in renal cell carcinoma. Cancer Res. 62, 4123–4131.

Cébe Suarez, S., Pieren, M., Cariolato, L., Arn, S., Hoffmann, U., Bogucki, A., Manlius, C., Wood, J., Ballmer-Hofer, K., 2006. A VEGF-A splice variant defective for heparan sulfate

and neuropilin-1 binding shows attenuated signaling through VEGFR-2. Cell. Mol. Life Sci. 63, 2067–77. doi:10.1007/s00018-006-6254-9

Chaitanya, G. V., Cromer, W.E., Parker, C.P., Couraud, P.O., Romero, I.A., Weksler, B., Mathis, J.M., Minagar, A., Alexander, J.S., 2013. A Recombinant Inhibitory Isoform of Vascular Endothelial Growth Factor164/165 Aggravates Ischemic Brain Damage in a Mouse Model of Focal Cerebral Ischemia. Am. J. Pathol. 183, 1010–1024. doi:10.1016/j.ajpath.2013.06.009

Cromer, W., Jennings, M.H., Odaka, Y., Michael Mathis, J., Steven Alexander, J., 2010. MURINE rVEGF164b, AN INHIBITORY VEGF REDUCES VEGF-A DEPENDENT ENDOTHELIAL PROLIFERATION AND BARRIER DYSFUNCTION. Microcirculation 17, no-no. doi:10.1111/j.1549-8719.2010.00047.x

Cromer, W.E., Ganta, C. V, Patel, M., Traylor, J., Kevil, C.G., Alexander, J., Mathis, J., 2013. VEGF-A isoform modulation in an preclinical TNBS model of ulcerative colitis: protective effects of a VEGF164b therapy. J. Transl. Med. 11, 207. doi:10.1186/1479-5876-11-207

Ferrara, N., 2010. Binding to the Extracellular Matrix and Proteolytic Processing: Two Key Mechanisms Regulating Vascular Endothelial Growth Factor Action. Mol. Biol. Cell 21, 687–690. doi:10.1091/mbc.e09-07-0590

Friedman, D.S., 2012. 2012 Fifth Edition Vision Problems in the U.S. Vis. Probl. U.S.

Kawamura, H., Li, X., Harper, S.J., Bates, D.O., Claesson-Welsh, L., 2008. Vascular endothelial growth factor (VEGF)-A165b is a weak in vitro agonist for VEGF receptor-2 due to lack of coreceptor binding and deficient regulation of kinase activity. Cancer Res. 68, 4683–4692. doi:10.1158/0008-5472.CAN-07-6577

Konopatskaya, O., Churchill, A.J., Harper, S.J., Bates, D.O., Gardiner, T.A., 2006. VEGF165b, an endogenous C-terminal splice variant of VEGF, inhibits retinal neovascularization in mice. Mol. Vis. 12, 626–632.

Li, Y.-L., Zhao, H., Ren, X.-B., 2016. Relationship of VEGF/VEGFR with immune and cancer cells: staggering or forward? Cancer Biol. Med. 13, 206–14. doi:10.20892/j.issn.2095-3941.2015.0070

Magnussen, A.L., Rennel, E.S., Hua, J., Bevan, H.S., Beazley Long, N., Lehrling, C., Gammons, M., Floege, J., Harper, S.J., Agostini, H.T., Bates, D.O., Churchill, A.J., Long, N.B., Lehrling, C., Gammons, M., Floege, J., Harper, S.J., Agostini, H.T., Bates, D.O., Churchill,

A.J., 2010. VEGF-A165b is cytoprotective and antiangiogenic in the retina. Invest. Ophthalmol. Vis. Sci. 51, 4273–4281. doi:10.1167/iovs.09-4296

Miller, J.W., Adamis, A.P., Aiello, L.P., 1997. Vascular endothelial growth factor in ocular neovascularization and proliferative diabetic retinopathy. Diabetes. Metab. Rev. 13, 37–50.

Nowak, D.G., Amin, E.M., Rennel, E.S., Hoareau-Aveilla, C., Gammons, M., Damodoran, G., Hagiwara, M., Harper, S.J., Woolard, J., Ladomery, M.R., Bates, D.O., 2010. Regulation of vascular endothelial growth factor (VEGF) splicing from pro-angiogenic to anti-angiogenic isoforms: a novel therapeutic strategy for angiogenesis. J. Biol. Chem. 285, 5532–40. doi:10.1074/jbc.M109.074930

Ourradi, K., Blythe, T., Jarrett, C., Barratt, S.L., Welsh, G.I., Millar, A.B., 2017. VEGF isoforms have differential effects on permeability of human pulmonary microvascular endothelial cells. Respir. Res. 18, 116. doi:10.1186/s12931-017-0602-1

Ozaki, H., Seo, M.S., Ozaki, K., Yamada, H., Yamada, E., Okamoto, N., Hofmann, F., Wood, J.M., Campochiaro, P.A., 2000. Blockade of vascular endothelial cell growth factor receptor signaling is sufficient to completely prevent retinal neovascularization. Am. J. Pathol. 156, 697–707. doi:10.1016/S0002-9440(10)64773-6

Park, J.E., Keller, G.A., Ferrara, N., 1993. The vascular endothelial growth factor (VEGF) isoforms: differential deposition into the subepithelial extracellular matrix and bioactivity of extracellular matrix-bound VEGF. Mol. Biol. Cell 4, 1317–1326. doi:10.1091/mbc.4.12.1317

Perrin, R.M., Konopatskaya, O., Qiu, Y., Harper, S., Bates, D.O., Churchill, A.J., 2005. Diabetic retinopathy is associated with a switch in splicing from anti- to pro-angiogenic isoforms of vascular endothelial growth factor. Diabetologia 48, 2422–2427. doi:10.1007/s00125-005-1951-8

Prahst, C., Heroult, M., Lanahan, A.A., Uziel, N., Kessler, O., Shraga-Heled, N., Simons, M., Neufeld, G., Augustin, H.G., 2008. Neuropilin-1-VEGFR-2 complexing requires the PDZ-binding domain of neuropilin-1. J. Biol. Chem. 283, 25110–25114. doi:10.1074/jbc.C800137200

Qiu, Y., Hoareau-Aveilla, C., Oltean, S., Harper, S.J., Bates, D.O., 2009. The anti-angiogenic isoforms of VEGF in health and disease. Biochem. Soc. Trans. 37, 1207–1213. doi:10.1042/BST0371207

Ritz, C., Baty, F., Streibig, J.C., Gerhard, D., 2015. Dose-response analysis using R. PLoS One 10, e0146021. doi:10.1371/journal.pone.0146021

Robbins, S.G., Conaway, J.R., Ford, B.L., Roberto, K.A., Penn, J.S., 1997. Detection of vascular endothelial growth factor (VEGF) protein in vascular and non-vascular cells of the normal and oxygen-injured rat retina. Growth Factors 14, 229–241.

Robinson, G.S., Pierce, E.A., Rook, S.L., Foley, E., Webb, R., Smith, L.E., 1996. Oligodeoxynucleotides inhibit retinal neovascularization in a murine model of proliferative retinopathy. Proc. Natl. Acad. Sci. U. S. A. 93, 4851–6. doi:10.1073/pnas.93.10.4851

Soker, S., Takashima, S., Miao, H.Q., Neufeld, G., Klagsbrun, M., 1998. Neuropilin-1 is expressed by endothelial and tumor cells as an isoform- specific receptor for vascular endothelial growth factor. Cell 92, 735–745. doi:10.1016/S0092-8674(00)81402-6

Taddei, A., Giampietro, C., Conti, A., Orsenigo, F., Breviario, F., Pirazzoli, V., Potente, M., Daly, C., Dimmeler, S., Dejana, E., 2008. Endothelial adherens junctions control tight junctions by VE-cadherin-mediated upregulation of claudin-5. Nat. Cell Biol. 10, 923–934. doi:10.1038/ncb1752

Ved, N., Hulse, R.P., Bestall, S.M., Donaldson, L.F., Bainbridge, J.W., Bates, D., 2017. Vascular endothelial growth factor-A 165 b ameliorates outer-retinal barrier and vascular dysfunction in the diabetic retina. Clin. Sci. CS20170102. doi:10.1042/CS20170102

Whitaker, G.B., Limberg, B.J., Rosenbaum, J.S., 2001. Vascular Endothelial Growth Factor Receptor-2 and Neuropilin-1 Form a Receptor Complex that is Responsible for the Differential Signaling Potency of VEGF165 and VEGF121. J. Biol. Chem. 276, 25520–25531. doi:10.1074/jbc.M102315200

Woolard, J., Wang, W.Y., Bevan, H.S., Qiu, Y., Morbidelli, L., Pritchard-Jones, R.O., Cui, T.G., Sugiono, M., Waine, E., Perrin, R., Foster, R., Digby-Bell, J., Shields, J.D., Whittles, C.E., Mushens, R.E., Gillatt, D.A., Ziche, M., Harper, S.J., Bates, D.O., 2004. VEGF165b, an inhibitory vascular endothelial growth factor splice variant: mechanism of action, in vivo effect on angiogenesis and endogenous protein expression. Cancer Res. 64, 7822–7835. doi:10.1158/0008-5472.CAN-04-0934

Xu, Q., Qaum, T., Adamis, A.P., 2001. Sensitive blood-retinal barrier breakdown quantitation using Evans blue. Invest. Ophthalmol. Vis. Sci. 42, 789–794.

Zhao, M., Shi, X., Liang, J., Miao, Y., Xie, W., Zhang, Y., Li, X., 2011. Expression of pro- and

anti-angiogenic isoforms of VEGF in the mouse model of oxygen-induced retinopathy. Exp. Eye Res. 93, 921–926. doi:10.1016/J.EXER.2011.10.013

Zhao, M., Xie, W.K., Bai, Y.J., Huang, L.Z., Wang, B., Liang, J.H., Yin, H., Li, X.X., Shi, X., 2015. Expression of total vascular endothelial growth factor and the anti□angiogenic VEGF165b isoform in the vitreous of patients with retinopathy of prematurity. Chin. Med. J. (Engl). 128, 2505–2509. doi:10.4103/0366-6999.164937

FIGURE LEGENDS

Figure 1. Primary retinal vein dilation following intra-vitreal injection of $VEGFA_{165}$a and $VEGFA_{165}$b.

Fluorescein angiography images of the same rat retinas pre-injection and 24 hours after injection with isoforms of $VEGFA_{165}$. Right (OD) eyes were injected with $VEGFA_{165}$ and contralateral (OS) eyes were injected with vehicle as controls. Both **A)** $VEGFA_{165}$a and **B)** $VEGFA_{165}$b caused visible dilation of the primary retinal veins using fluorescein angiography after 24 hours. Vehicle injected control eyes did not show vein dilation.

Figure 2. Induction and recovery of primary retinal vein dilation following intra-vitreal injection of $VEGFA_{165}$b.

Fluorescein angiography and SD-OCT images of the same a rat retina pre- and post-injection (24 and 72 hours). (Dose 250 ng/eye) One of the five primary veins is labeled (v) at each time point in the fluorescein and OCT images. Primary veins have larger diameters than the arteries. **A)** Fluorescein angiography images. All five primary retinal veins displayed a visible dilation at 24 hours post-injection. Recovery to pre-injection diameter was essentially complete by 72 hours post-injection. **B)** SD-OCT *en face* views of primary vessel shadows for the same retina. Green horizontal lines indicate the location of OCT cross-sectional images shown below. Arrows indicate the location of the cross sectional OCT views. **C)** Zoomed view of OCT cross-sectional images with digital-calipers to measure the diameter of the vein at the location (v) in panel B).

Figure 3. Aflibercept blocks primary retinal vein dilation caused by intravitreal injection of $VEGFA_{165}$b.

Fluorescein angiography of the OD eye, showing the dilation of primary retinal veins 24 hours post injection with $VEGFA_{165}$**b** (white arrows). Significant recovery from the transient dilation is seen at 48 hours post-injection. Co-injection of Aflibercept with $VEGFA_{165}$**b**, in the OS eye, blocked the dilation effect.

Figure 4. Changes in diameter of primary retinal veins by $VEGFA_{165}$ isoforms *in vivo*.
Animals received intravitreal injections in one eye with either $VEGFA_{165}$a or $VEGFA_{165}$b (300ng). The contralateral eye received an intravitreal injection with PBS (vehicle) only. At 24 hours post-injection, all retinas were reimaged and vein diameters were re-measured at the same locations. (**p<0.005 vs vehicle. *p<0.03 vs vehicle, N=2 rats per isoform)

Figure 5. Retinal thickness changes induced by $VEGFA_{165}$a or $VEGFA_{165}$b.
Retinal thickness was measured from SD-OCT data, between the Inner-Limiting Membrane (ILM) and the Outer-Limiting Membrane (OLM). Total thickness was averaged from 24-grid locations centered on the optic disc and including the central to mid retina. Central thickness was averaged from 8/24 locations adjacent to the optic disc. Mid thickness was averaged from 16/24 locations more peripheral to the optic disc. **A)** $VEGFA_{165}$a caused a relative increase in retinal thickness compared to PBS-injected contralateral eyes measured over the total area (P<0.05), central area (P<0.05) and mid area (P<0.05). **B)** $VEGFA_{165}$b also caused a relative increase in thickness compared to PBS-injected contralateral eyes for the total area (P<0.05), central area (P<0.001) and mid area (P<0.05). (t-test, N=2 rats per group)

Figure 6. Effect of $VEGFA_{165}$ isoforms intravenous Evans Blue dye leakage into the vitreous humor *in vivo*.
Both eyes of Long Evans rats were first imaged by fluorescein angiography before intravitreal injection of VEGFA isoforms (pre-injection fluorescein). After a week of recovery, rats received intravitreal injections of the a-isoform or b-isoform in the OD eye and injection with vehicle (PBS) in the OS eye. 22-hours post-VEGFA injections, animals received an intravenous injection of Evans Blue dye. Two hours later, rat's eyes were imaged by Evans Blue angiography (24 hour Evans Blue). **A)** Treatment with $VEGFA_{165}$a increased permeability of the vasculature compared to PBS-only. Strong intravitreal Evans Blue fluorescence (OD) overwhelmed the ability to visualize the retinal vasculature, which was imaged clearly in the PBS-injected eyes (OS). **B)** Treatment with $VEGFA_{165}$b (OD) also resulted in the appearance of more Evan's blue fluorescence in the vitreous compared to contralateral (OS) PBS-injected eyes.

Figure 7. Activation of MAPK and AKT in HRMECs by $VEGFA_{165}$a and $VEGFA_{165}$b

A) Immunoblots of total MAPK and activated MAPK (Phospho-MAPK) 10 minutes after treatment with $VEGFA_{165}$a (Va), $VEGFA_{165}$b (Vb), or media control (C). Two representative experiments are shown. **B)** Immunoblots of total AKT and activated AKT (Phospho-AKT) 10 minutes after treatment with $VEGFA_{165}$a (Va), $VEGFA_{165}$b (Vb), or media control (C). Two representative experiments are shown. **C)** Fold activation of MAPK and AKT from three immunoblotting experiments. P-values are shown, t-test relative to media controls (1-fold).

Figure 8. Activation of MAPK in primary HRMECs by isoforms of $VEGFA_{165}$.

Activation of MAPK was measured by *in-situ* immunofluorescence with a phospho-specific antibody (phospho-Thr202/Tyr204) for p44/42. **A)** Activation of MAPK at three time-points after the addition of 100 pM $VEGFA_{165}$a or $VEGFA_{165}$b. Bar shows standard deviation. (t-test, *** $p<0.001$ relative to untreated control, n=8 biological replicates.) **B)** Dose-response curves for activation of MAPK. The ED_{50} was 73 pM for $VEGFA_{165}$a and 1015 pM for $VEGFA_{165}$b. Bars indicate the 95% confidence interval for data fit to the 4-parameter log-logistic dose-response function. N=4 biological replicates per dose.

Figure 9. Activation of AKT in primary HRMECs by isoforms of $VEGFA_{165}$.

A) Activation of AKT was measured by *in-situ* immunofluorescence with a phospho-specific antibody for Ser473-AKT at five time-points after the addition of 20 ng/mL (1,250 pM) $VEGFA_{165}$a or $VEGFA_{165}$b. Bar shows standard deviation. (t-test, ***$p<0.001$ relative to untreated control, n=4 biological replicates.) **B)** Dose response curves for activation of AKT. The ED_{50} value for AKT activation by $VEGFA_{165}$a was 53 pM compared to 126 pM for $VEGFA_{165}$b. Bars indicate the 95% confidence interval for data fit to the 4-parameter log-logistic dose-response function. N=4 biological replicates per dose.

Figure 10. Dose-response curves for activation of VEGFR2 by isoforms of $VEGFA_{165}$.

The a-isoform was a stronger activator of VEGFR2 compared to the b-isoform. The ED_{50} for activation by $VEGFA_{165}$a was 254 pM compared to 1192 pM for $VEGFA_{165}$b. Bars indicate the 95% confidence interval for data fit to the 4-parameter log-logistic dose-response function. N=4 biological replicates per dose.

Figure 11. Effects of $VEGFA_{165}$ isoforms on expression of leukocyte-endothelial cell adhesion genes in HRMECs.

A) *ICAM1* gene expression at 1, 3, 6 and 24 hours after $VEGFA_{165}$ treatment. Confluent HRMECs were treated with 100 ng/mL (5,300 pM) of $VEGFA_{165}$a or $VEGFA_{165}$b. **B)** *ICAM1* gene expression comparing $VEGFA_{165}$a and $VEGFA_{165}$b at a low, intermediate and high dose measured after 6-hours. **C)** *Selectin-E* gene expression at 1, 3, 6 and 24 hours after $VEGFA_{165}$ treatment. **D)** *Selectin-E* gene expression comparing $VEGFA_{165}$a and $VEGFA_{165}$b at a low, intermediate and high dose measured after 6-hours. **E)** *VCAM1* gene expression at 1, 3, 6 and 24 hours after $VEGFA_{165}$ treatment. **F)** *VCAM1* gene expression comparing $VEGFA_{165}$a and $VEGFA_{165}$b at a low, intermediate and high dose measured after 6-hours. (For all graphs, t-test relative to media controls: *p<0.05, **p<0.01, ***p<0.001, triplicate assays.)

Figure 12. Effects of $VEGFA_{165}$ isoforms on the expression of tight-junction genes in HRMECs.

A) *Claudin-5* gene expression at 1, 3, 6 and 24 hours after $VEGFA_{165}$ treatment. Confluent HRMECs were treated with 100 ng/mL (5,300 pM) of $VEGFA_{165}$a or $VEGFA_{165}$b. **B)** *Claudin-5* gene expression comparing $VEGFA_{165}$a and $VEGFA_{165}$b at a low, intermediate and high dose measured after 6-hours. **C)** *Occludin* gene expression at 1, 3, 6 and 24 hours after $VEGFA_{165}$ treatment. **D)** *Occludin* gene expression comparing $VEGFA_{165}$a and $VEGFA_{165}$b at a low, intermediate and high dose measured after 6-hours. (For all graphs, t-test relative to media controls: *p<0.05, **p<0.01, ***p<0.001, triplicate assays.)

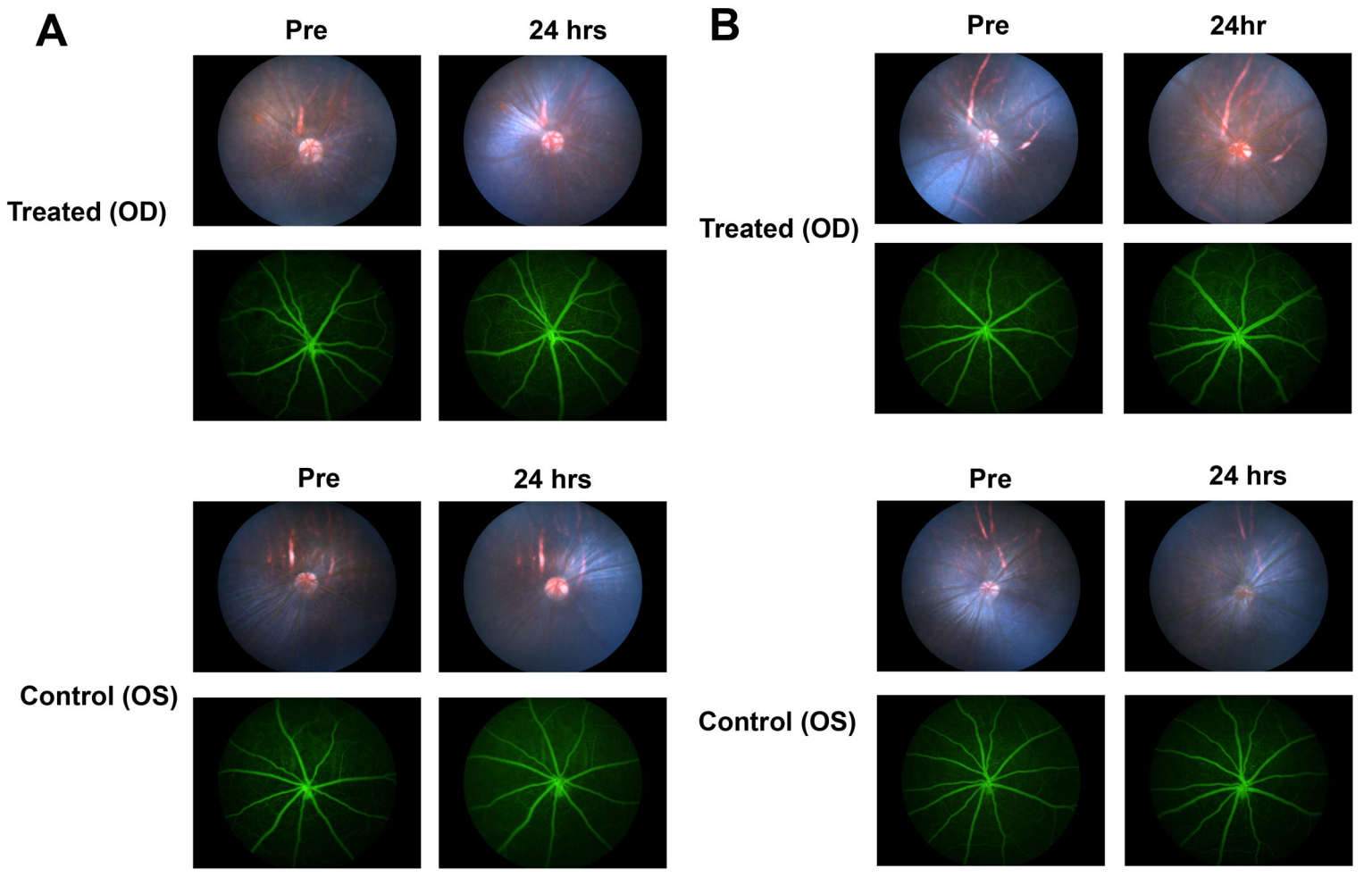
A
Pre
24 hrs
Treated (OD)
Pre
24 hrs
Control (OS)
B
Pre
24hr
Treated (OD)
Pre
24 hrs
Control (OS)

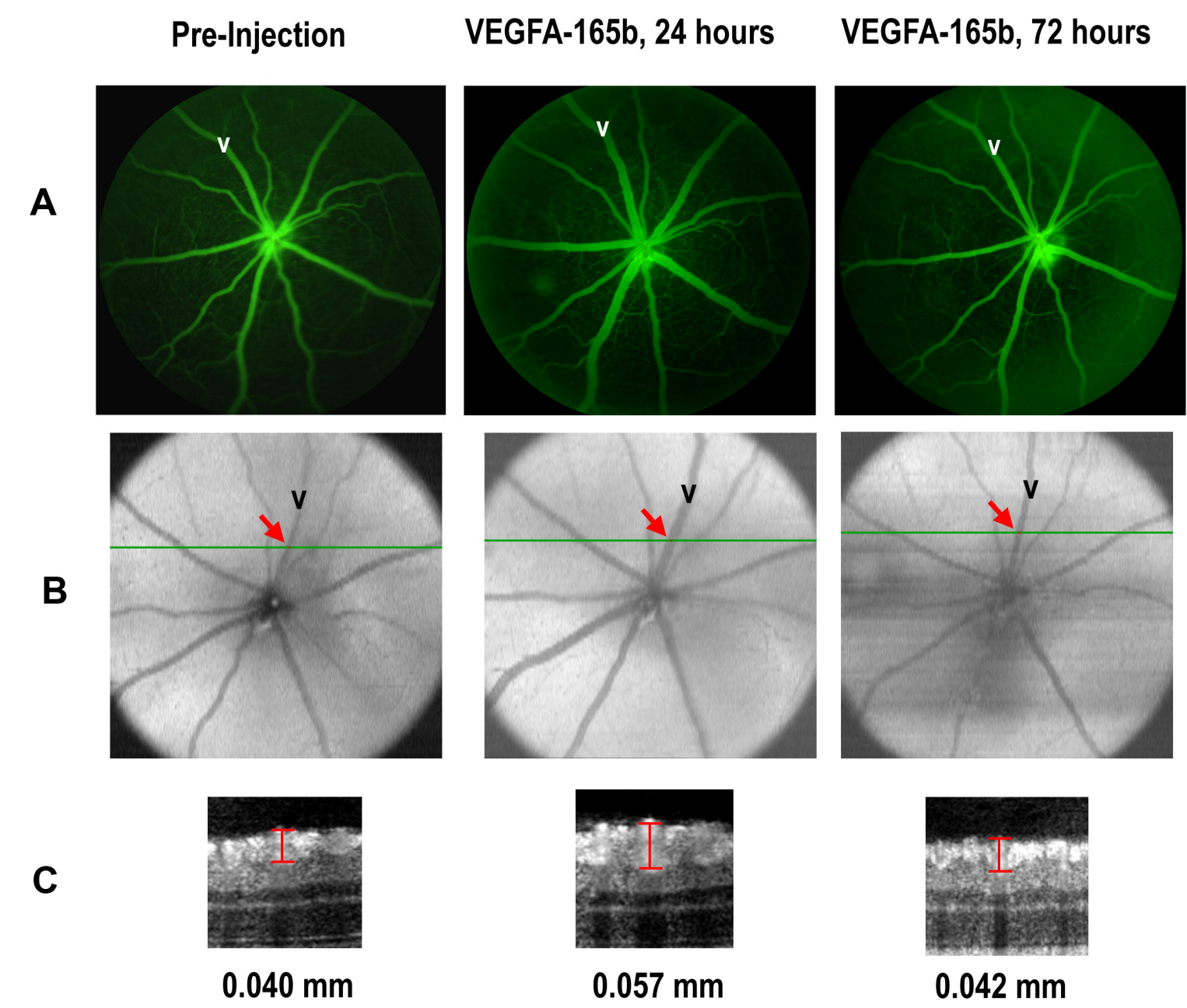
Pre-Injection
VEGFA-165b, 24 hours
VEGFA-165b, 72 hours
A
B
C
V
V
V
V
V
V
0.040 mm
0.057 mm
0.042 mm

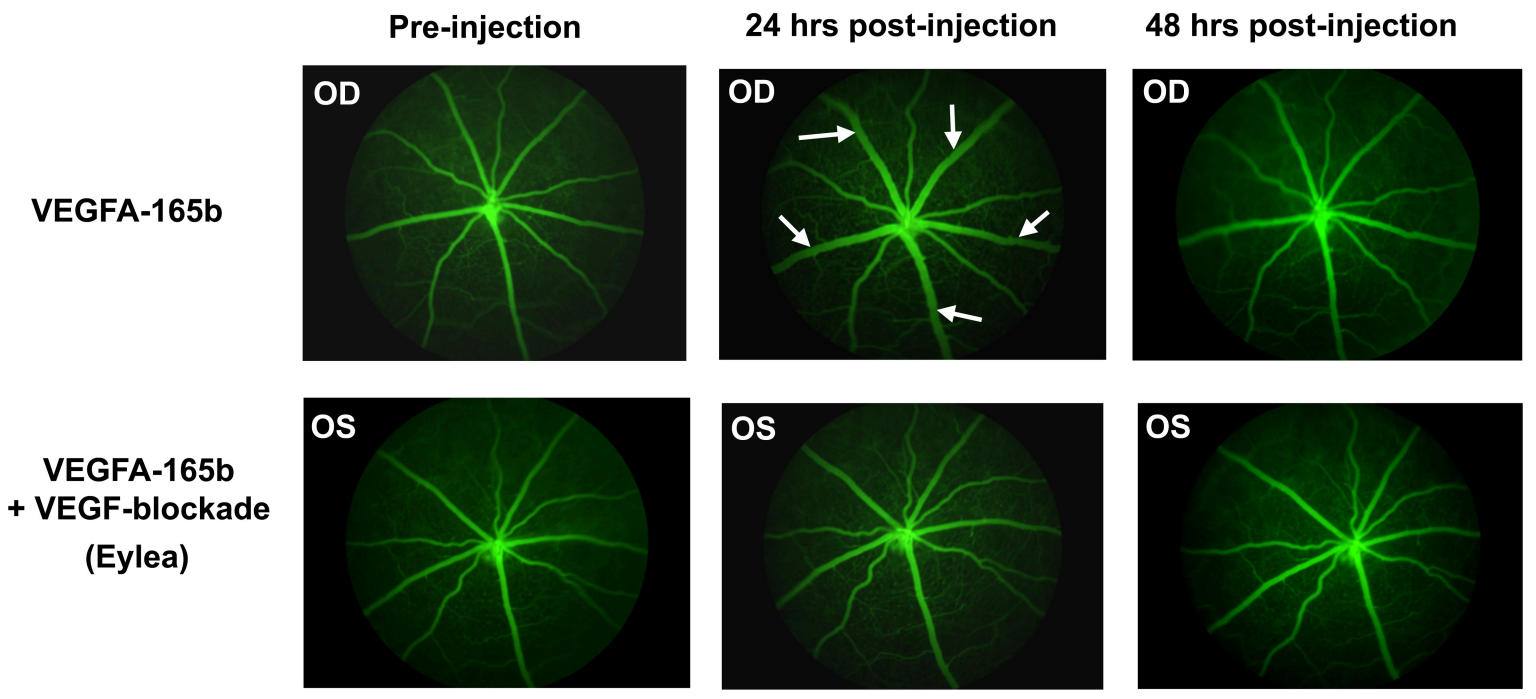
Pre-injection
24 hrs post-injection
48 hrs post-injection
VEGFA-165b
OD
OD
OD
VEGFA-165b
+ VEGF-blockade
(Eylea)
OS
OS
OS

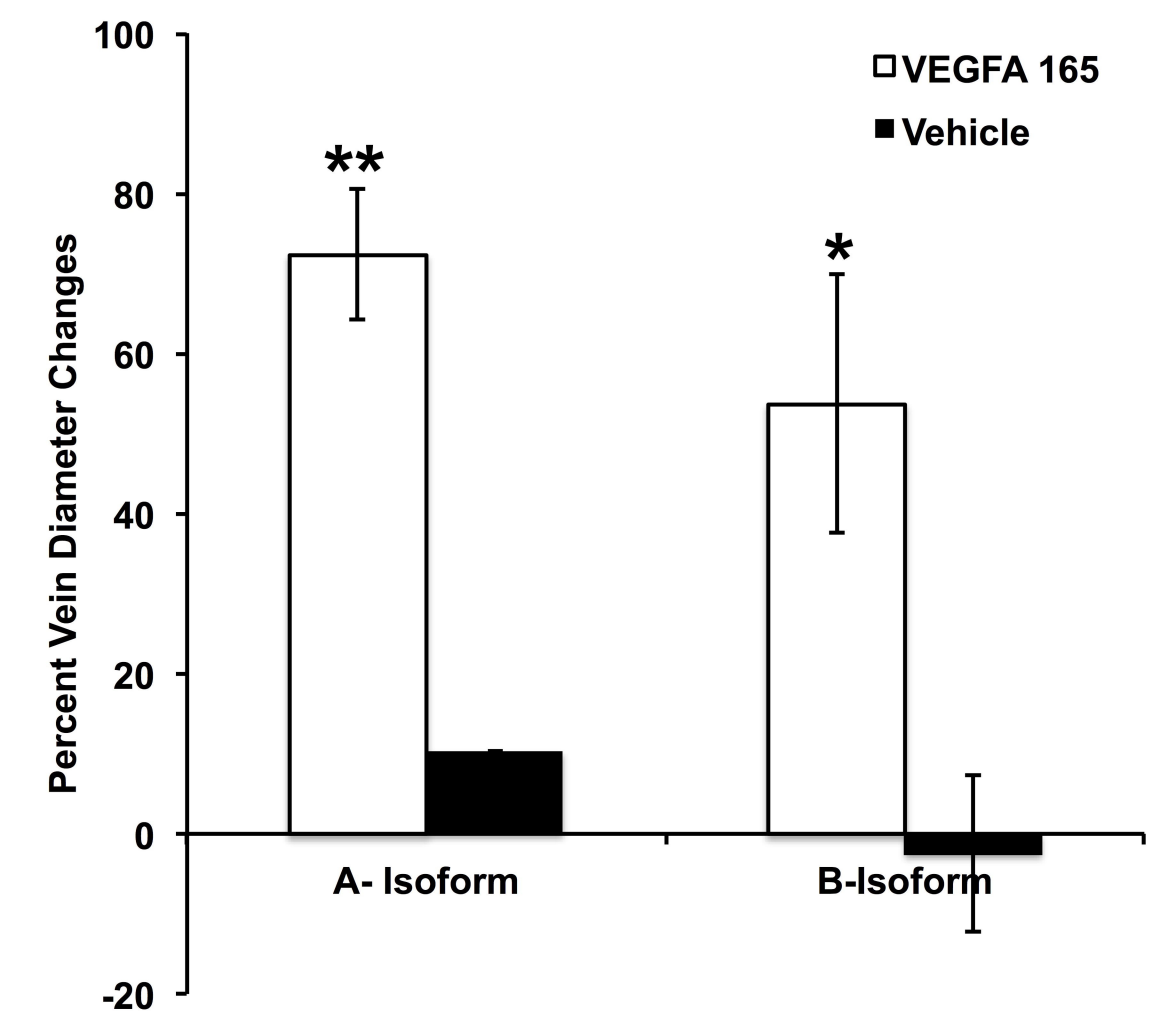
100
80
60
40
20
0
-20
Percent Vein Diameter Changes
VEGFA 165
Vehicle
**
*
A- Isoform
B-Isoform

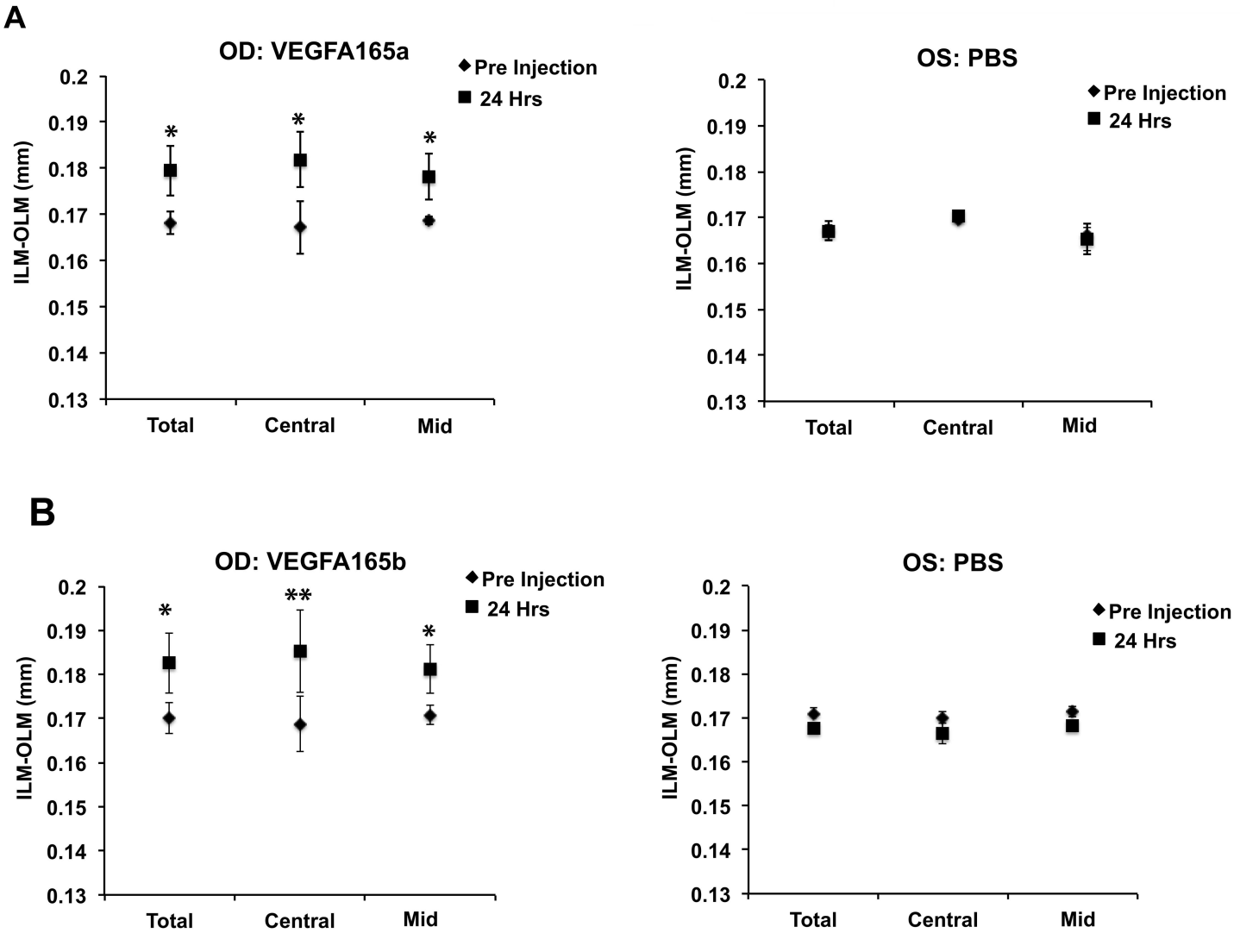
A
OD: VEGFA165a
Pre Injection
24 Hrs
ILM-OLM (mm)
0.2
0.19
0.18
0.17
0.16
0.15
0.14
0.13
*
*
*
Total
Central
Mid
OS: PBS
Pre Injection
24 Hrs
ILM-OLM (mm)
Total
Central
Mid
B
OD: VEGFA165b
Pre Injection
24 Hrs
ILM-OLM (mm)
*
**
*
Total
Central
Mid
OS: PBS
Pre Injection
24 Hrs
ILM-OLM (mm)
Total
Central
Mid

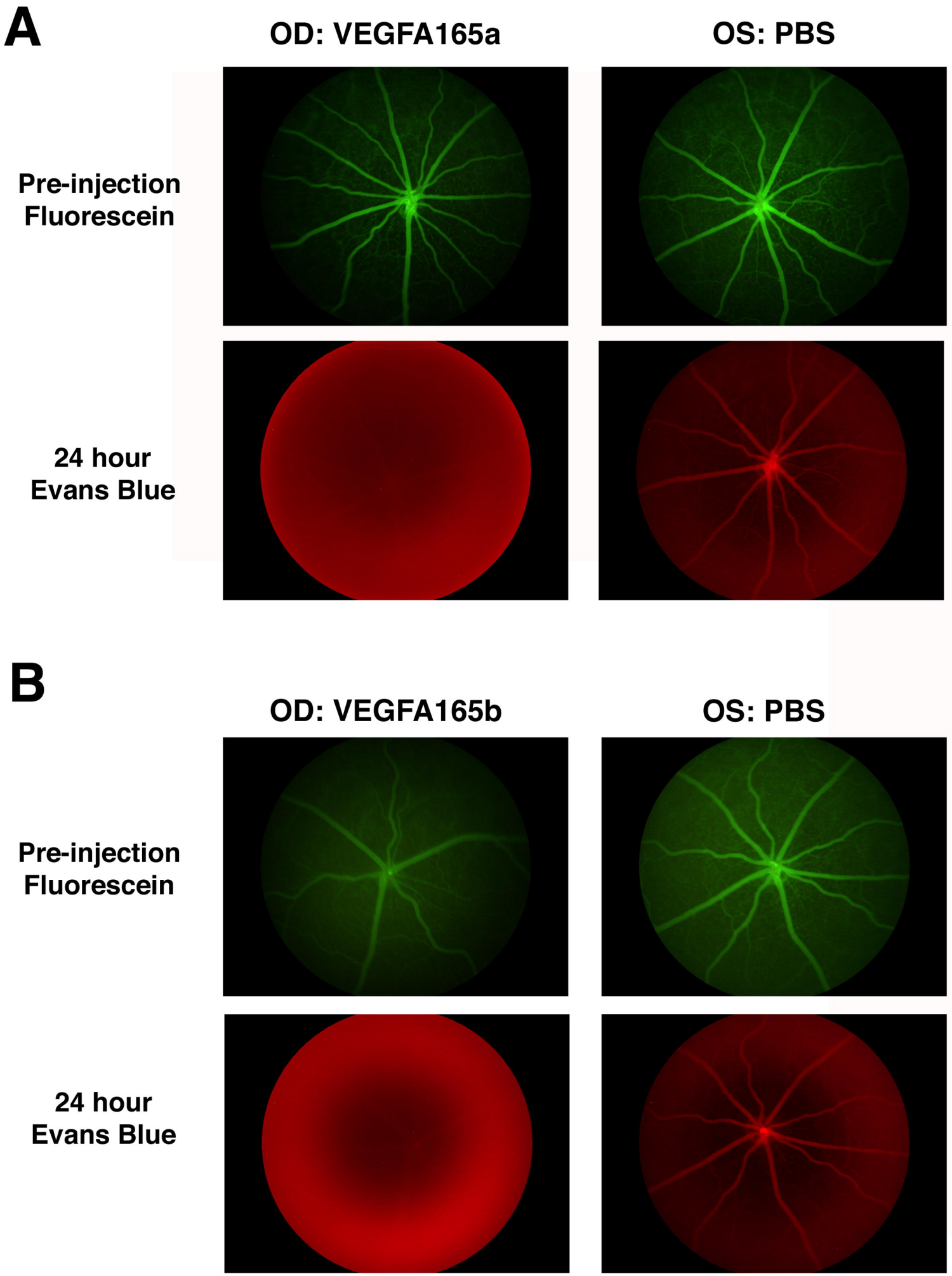
A
OD: VEGFA165a
OS: PBS
Pre-injection Fluorescein
24 hour Evans Blue
B
OD: VEGFA165b
OS: PBS
Pre-injection Fluorescein
24 hour Evans Blue

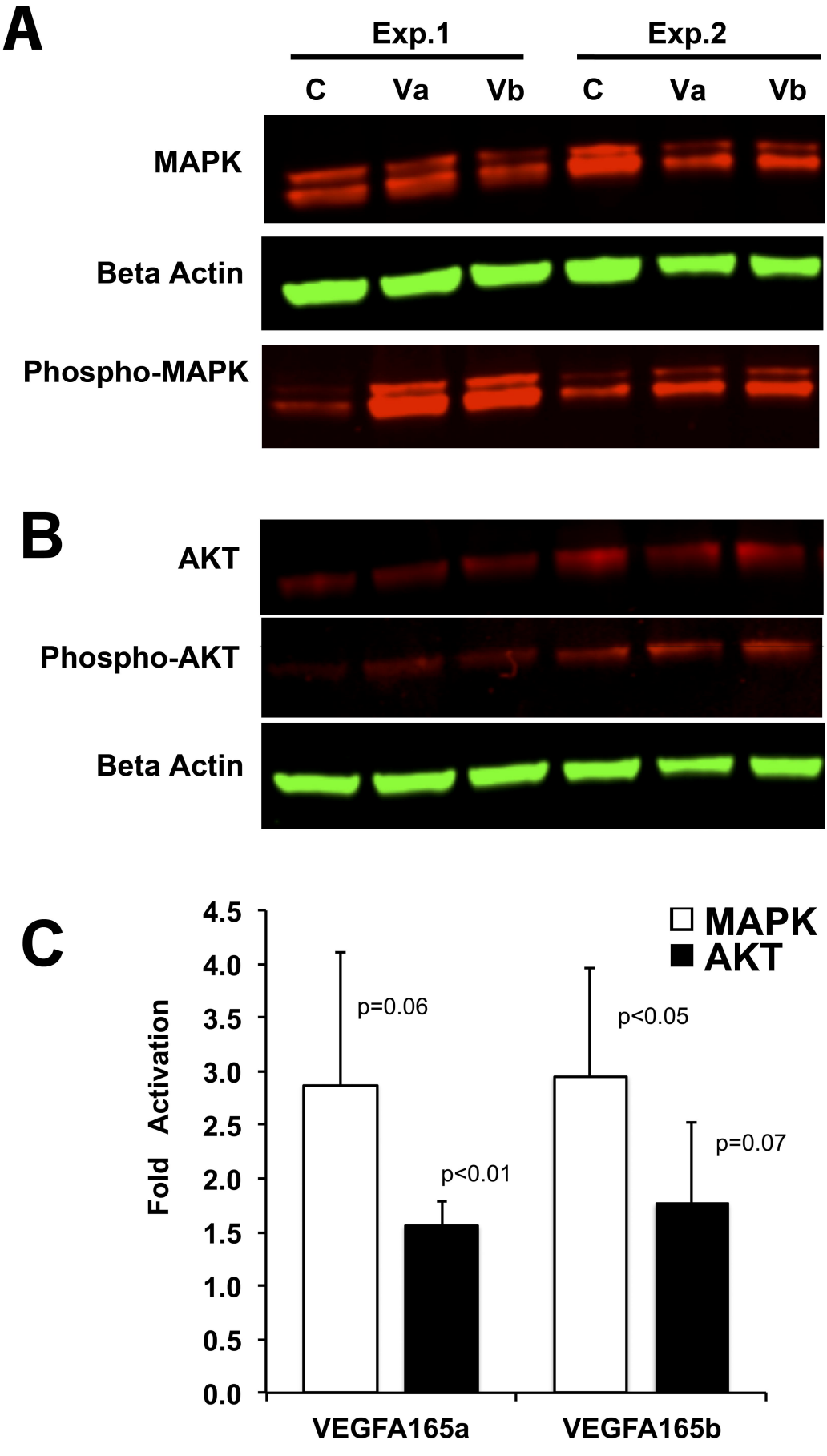
A
Exp.1
Exp.2
C
Va
Vb
C
Va
Vb
MAPK
Beta Actin
Phospho-MAPK
B
AKT
Phospho-AKT
Beta Actin
C
MAPK
AKT
Fold Activation
4.5
4.0
3.5
3.0
2.5
2.0
1.5
1.0
0.5
0.0
p=0.06
p<0.01
p<0.05
p=0.07
VEGFA165a
VEGFA165b

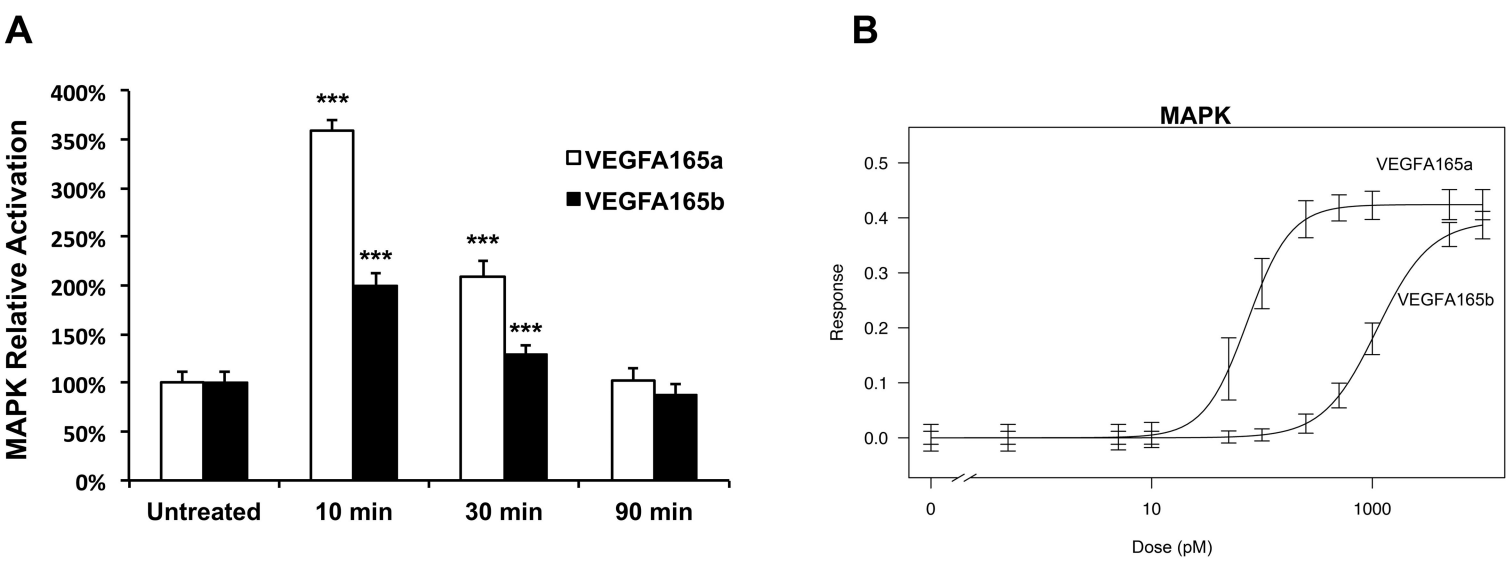
A
MAPK Relative Activation
400%
350%
300%
250%
200%
150%
100%
50%
0%
***
***
***
***
VEGFA165a
VEGFA165b
Untreated
10 min
30 min
90 min
B
MAPK
VEGFA165a
VEGFA165b
Response
0.5
0.4
0.3
0.2
0.1
0.0
0
10
1000
Dose (pM)

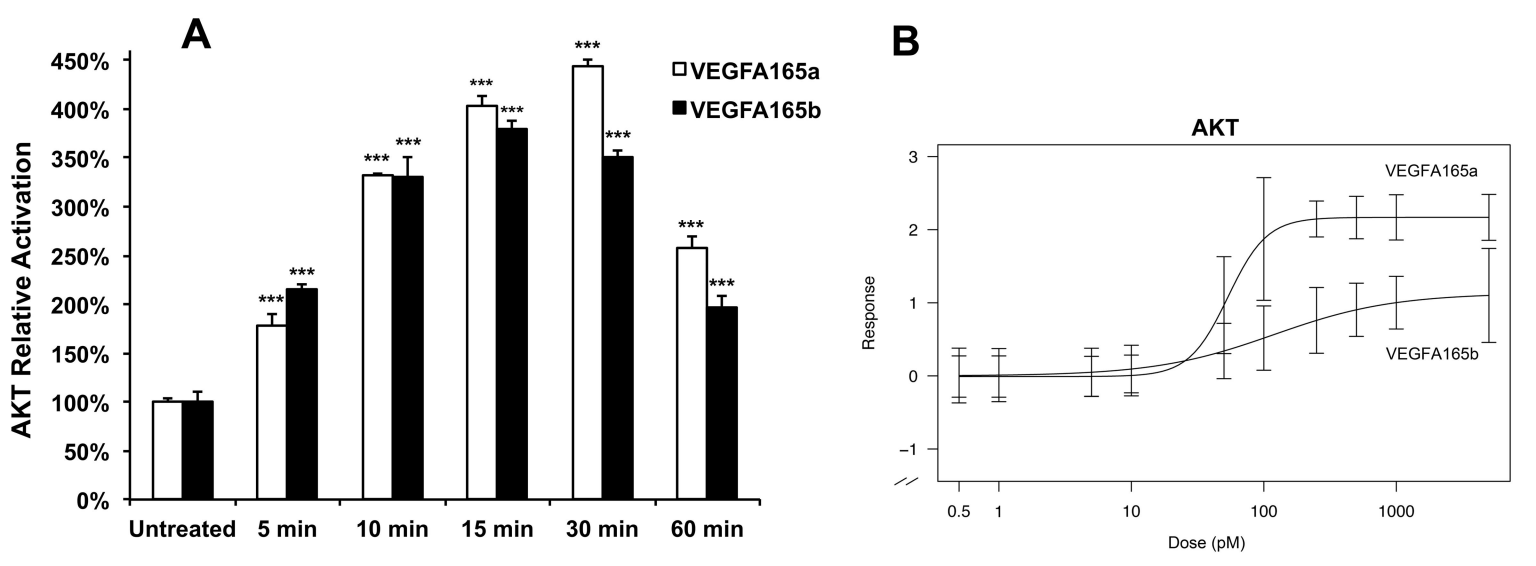
A
AKT Relative Activation
450%
400%
350%
300%
250%
200%
150%
100%
50%
0%
VEGFA165a
VEGFA165b
***
Untreated
5 min
10 min
15 min
30 min
60 min
B
AKT
VEGFA165a
VEGFA165b
Response
3
2
1
0
−1
0.5
1
10
100
1000
Dose (pM)

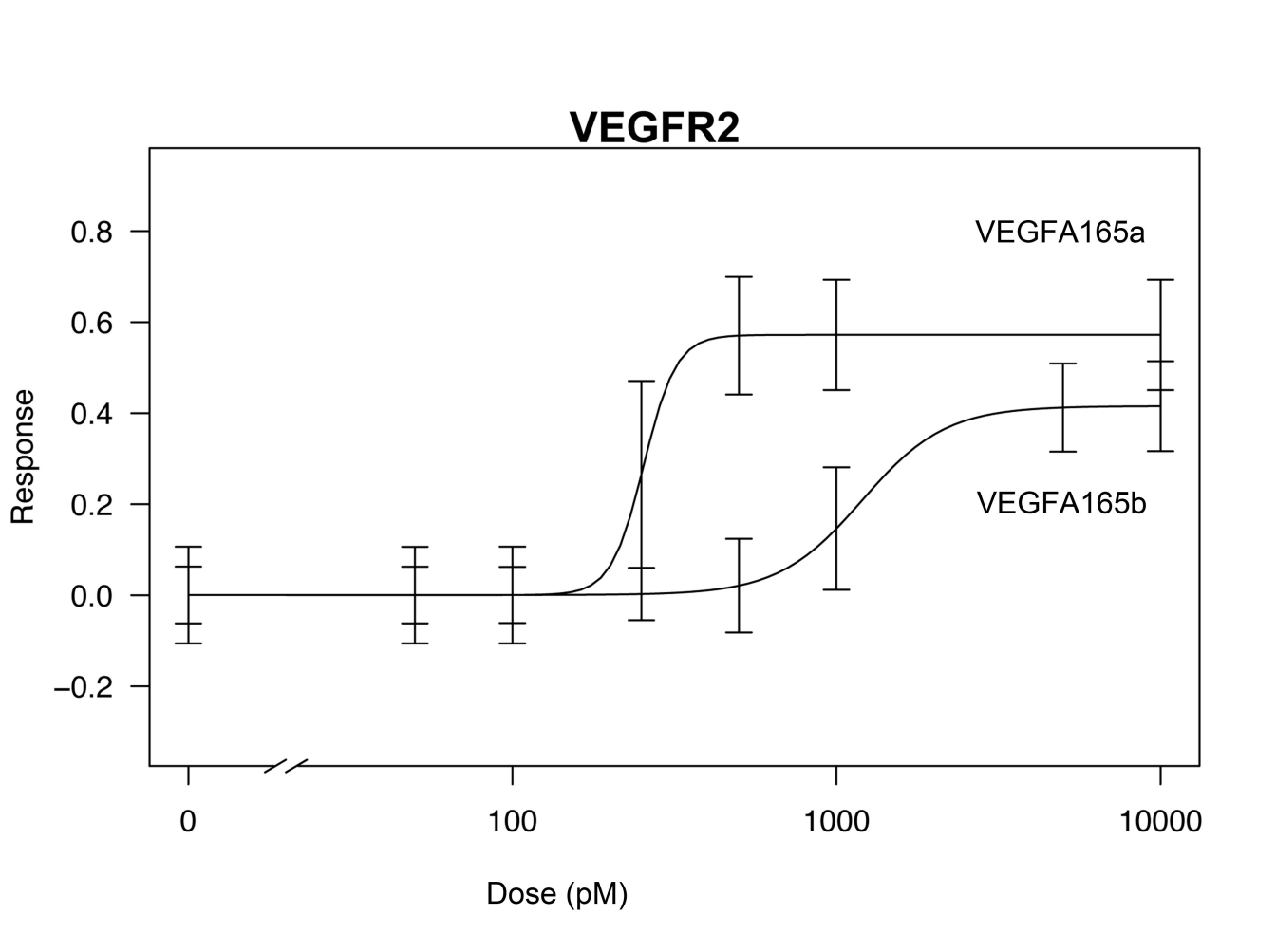
VEGFR2
VEGFA165a
VEGFA165b
Response
0.8
0.6
0.4
0.2
0.0
−0.2
0
100
1000
10000
Dose (pM)

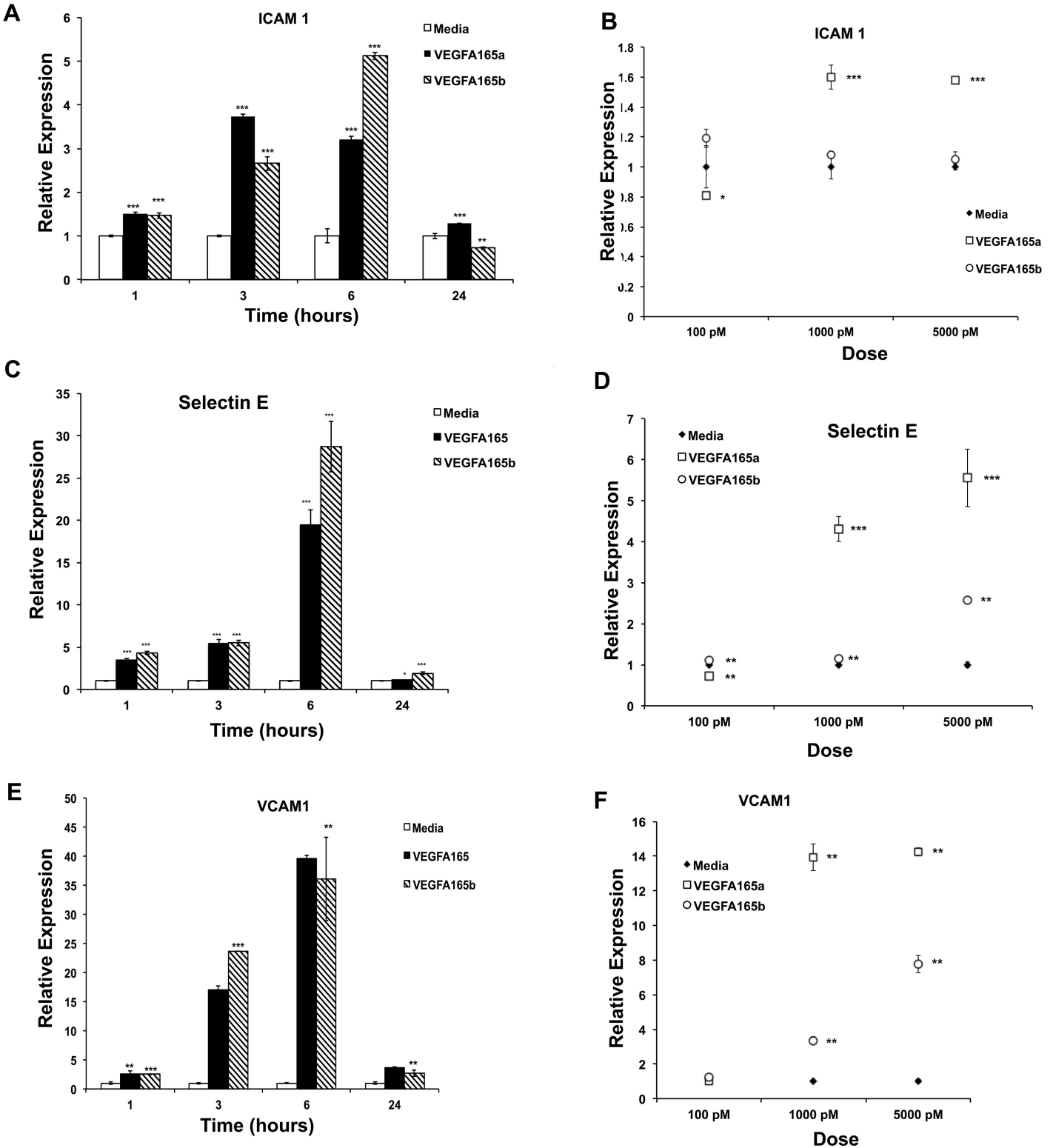
A
ICAM 1
Media
VEGFA165a
VEGFA165b
Relative Expression
Time (hours)
B
ICAM 1
Media
VEGFA165a
VEGFA165b
Relative Expression
100 pM
1000 pM
5000 pM
Dose
C
Selectin E
Media
VEGFA165
VEGFA165b
Relative Expression
Time (hours)
D
Selectin E
Media
VEGFA165a
VEGFA165b
Relative Expression
100 pM
1000 pM
5000 pM
Dose
E
VCAM1
Media
VEGFA165
VEGFA165b
Relative Expression
Time (hours)
F
VCAM1
Media
VEGFA165a
VEGFA165b
Relative Expression
100 pM
1000 pM
5000 pM
Dose

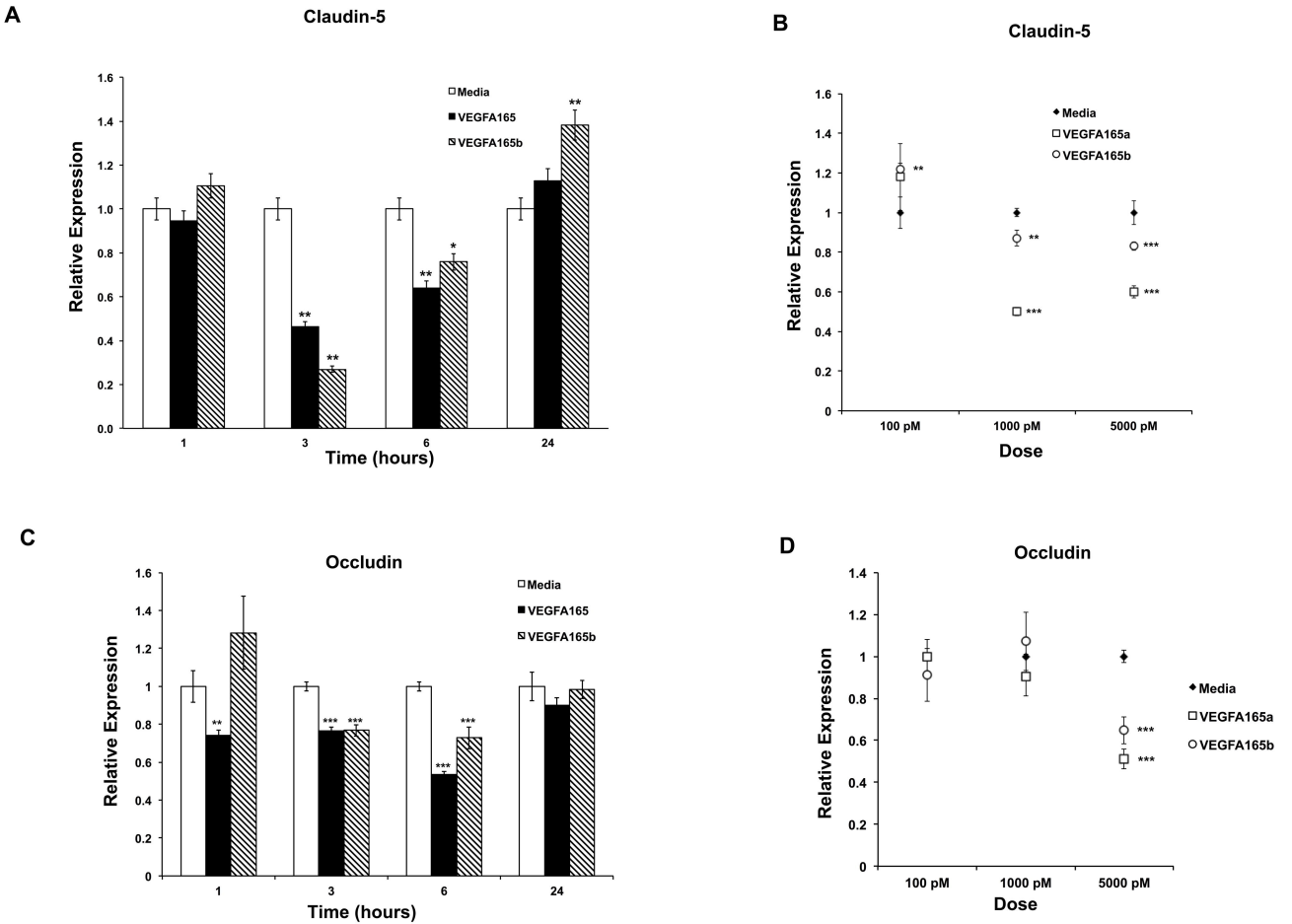
A
Claudin-5
Relative Expression
Time (hours)
Media
VEGFA165
VEGFA165b
B
Claudin-5
Relative Expression
Dose
Media
VEGFA165a
VEGFA165b
100 pM
1000 pM
5000 pM
C
Occludin
Relative Expression
Time (hours)
Media
VEGFA165
VEGFA165b
D
Occludin
Relative Expression
Dose
Media
VEGFA165a
VEGFA165b
100 pM
1000 pM
5000 pM